

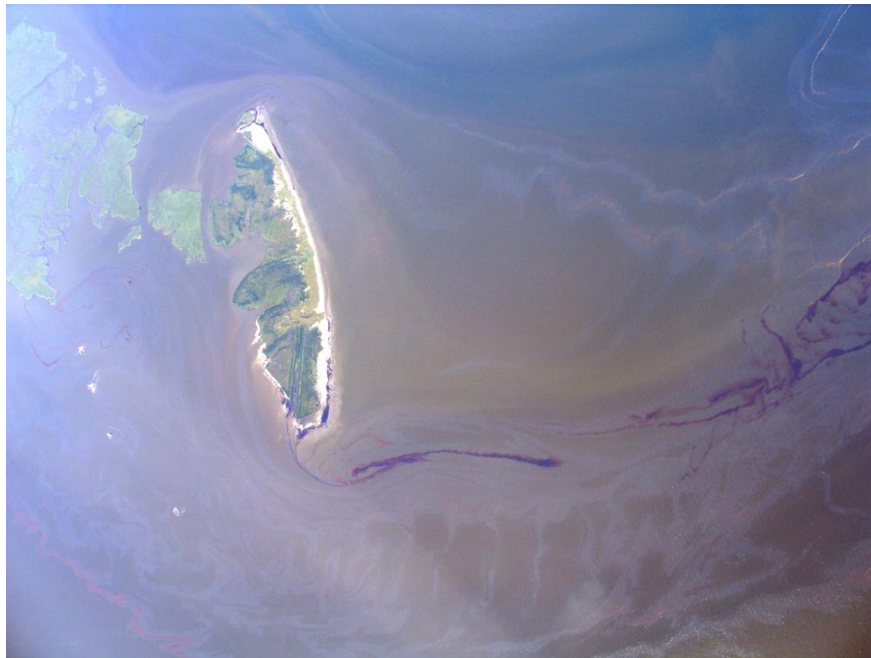
# **Open Water Multispectral Aerial Sensor Oil Spill Thickness Mapping in Arctic and High Sediment Load Conditions.**

## **Final Report**

Submitted to the U.S. Department of the Interior  
Bureau of Safety and Environmental Enforcement  
(Formerly Bureau of Ocean Energy Management, Regulation and Enforcement)  
Herndon, VA

31 October, 2012  
Revised 19 November, 2012

Contract No. E12PC0002 (Re-obligated Contract No.M10PC00068)



**Principal Investigator:** Dr. Jan Svejksky, Ocean Imaging Corp. 201 Lomas Santa Fe Dr.,  
Suite 370, Solana Beach, CA 92075 (858) 792-8529, Fax: (858) 792-8761, [jan@oceani.com](mailto:jan@oceani.com)

**Co-Investigator:** Judd Muskat, CDFG Office of Oil Spill Prevention and Response, 1700 "K"  
Street, Sacramento, CA 95814 (916) 324-3411, [jmuskat@ospr.dfg.ca.gov](mailto:jmuskat@ospr.dfg.ca.gov)

## **Acknowledgement**

This project is funded by the Bureau of Safety and Environmental Enforcement (BSEE). The authors wish to thank BSEE for funding this study and Joseph Mullin for his guidance in the work. Thanks also go to the California Department of Fish and Game, Office of Oil Spill Prevention and Response for providing the plane and pilot for some of the remote sensing experiments and hardware tests, and to the staff of the Ohmsett Facility for their assistance in conducting cold weather tests at Ohmsett in February, 2010 and October, 2011.

## **Disclaimer**

This report has been reviewed by BSEE staff for technical adequacy according to contractual specifications. The opinions, conclusions, and recommendations contained in the report are those of the author and do not necessarily reflect the views and policies of BSEE. The mention of a trade name or any commercial product in the report does not constitute an endorsement or recommendation for use by BSEE. Finally, this report does not contain any commercially sensitive, classified or proprietary data release restrictions and may be freely copied and widely distributed.

***On the Cover:** An island within the highly turbid waters of the Mississippi River Delta, Louisiana, surrounded by oil slicks of various thicknesses from the Deepwater Horizon oil spill.*

# TABLE OF CONTENTS

<b>EXECUTIVE SUMMARY</b>	1
<b>1. PROJECT BACKGROUND</b>	
1.1 Present-day Oil Spill Assessment Techniques	3
1.2 Project's Objectives and Approach	4
<b>2. PROJECT RESULTS</b>	5
2.1 Task 1 – Determination & Initial Testing of Arctic Region-suitable Digital Dissemination System	5
2.2 Task 2 – Wintertime Testing of Oil Thickness Mapping Sensor at Ohmsett	5
2.3 Task 3 – Cold Environment IR Thickness Algorithm Development	7
2.4 Task 4 – Development of Simplified Multispectral System	7
2.5 Task 5 – System Testing in Alaska	8
2.6 Task 6 – System Testing in Highly Turbid Waters (Gulf of Mexico)	9
2.7 Task 7 – Determination of visible-nearIR and thermal IR response characteristics using imagery acquired during the Deepwater Horizon Oil Spill	11
2.8 Task 8 – Initial Oil Emulsion Characterization Algorithm Development	13
2.9 Task 9 – Controlled Oil Emulsion Data Acquisition and Initial Approach Testing at Ohmsett	14
2.10 Task 10 – Advanced Algorithm Development	16
2.11 Task 11 – Emulsion Mapping System Tests over Santa Barbara Oil Seeps	17
<b>3. PUBLICATION OF RESULTS</b>	21
<b>4. REFERENCES</b>	21
<b>5. APPENDIX A (News article from the Arctic Sounder)</b>	23
<b>6. APPENDIX B (Debrief from Chevron Oil Drill)</b>	26
<b>7. APPENDIX C (PE&amp;RS October 2012 Cover Article)</b>	29

## EXECUTIVE SUMMARY

This project represents an expanded follow-on effort aimed to develop a hardware/software system that would enable near-real-time mapping of an at-sea oil spill and its thickness distributions. The initial work, funded by the Minerals Management Service (MMS), targeted the development of an algorithm that would enable the measurement of oil slick thicknesses using multispectral aerial imagery and evaluation of the feasibility of developing a relatively economical, portable aerial oil spill mapping system that could be operationally deployed. Such a system would enable rapid oil spill mapping with greater quantitative and geographical accuracy than is possible using visual observations. The California Department of Fish and Game's Office of Oil Spill Prevention and Response (CDFG/OSPR) partnered with MMS on the project and provided technical expertise with the project's Geographic Information System (GIS) components as well as services in kind (plane and pilot). An oil thickness measurement algorithm was developed that utilized 4 customized wavelengths in the visible range from a multispectral aerial sensor. A thermal infrared (IR) imager was also added to the system following further research. Using data obtained under small-scale laboratory conditions, larger-scale experiments at Ohmsett (the National Oil Spill Response Test Facility in Leonardo, New Jersey), and aerial and ship-based field sampling of slicks from natural oil seeps in California's Santa Barbara Channel, the oil thickness algorithm was developed and validated for light and medium weight crudes and several IFOs.

Due to spectral reflectance properties of these oils the usable thickness range of the UV-visible-nearIR wavelength imaging proved to be from sheens to approximately 0.15-0.2mm. Thicker oil films could still be positively identified and their distribution mapped but their true thickness could no longer be distinguished. The addition of the thermalIR imager expanded the initial algorithm's effective thickness measurement range to several millimeters. The thermal imager also proved to allow the mapping of refined petroleum products such as diesel, jet fuel and lubricant oils that have no distinct color reflectance characteristics at thicknesses usually encountered in an at-sea or harbor spill. The thermal imaging also added nighttime mapping capabilities. During its development, the system was utilized experimentally by OSPR during the M/V *Cosco Busan* oil spill in San Francisco in November, 2007. The system was successfully utilized in full operational mode during a platform spill in the Santa Barbara Channel in December, 2008 and another small spill (M/V *Dubai Star*) in San Francisco Bay in October, 2009.

The present project addressed continued development and testing related to enabling the use of the oil spill mapping system over waters with very high suspended sediment loads (such as near river deltas, shallow regions with strong vertical mixing, etc.) and under freezing or near freezing water and air temperatures. High turbidity conditions were expected to affect oil sensing algorithms using UV-visible-nearIR wavelengths, while cold temperatures could affect oil signature behavior in the thermal IR imagery. Experiments at Ohmsett during February, 2010 provided the needed data to expand the existing oil thickness mapping algorithms to cover low air/water temperature conditions. Data for examining the effects of high turbidity were acquired during Ocean Imaging's (OI's) extensive operational work in support of response operations during the Deepwater

Horizon spill in the Gulf of Mexico. OI staff conducted one to two imaging missions almost daily for 3 months in the summer of 2010 and had multiple opportunities to obtain the needed data when the oil reached the very turbid waters surrounding the Mississippi River delta. Analysis of these data allowed further refinements to the mapping algorithms to adjust for such extreme water color conditions.

Another objective of this on-going project was to evaluate available hardware options for inclusion in a second generation system that would be even more compact and portable, and simpler to operate by a non-expert. Such a system could then be potentially owned and operated by regional agencies, allowing very rapid deployment and utilization when needed. The most simplification can be accomplished by replacing the existing 4-camera multispectral instrument covering the visible-nearIR wavelength range with a single lens, multi-CCD camera that uses a specialized image-splitting prism and auxiliary filters to create a 4 to 5 channel imager that is very compact and simple to integrate into the entire system. Additionally, OI investigated and field-tested several options for disseminating the image data from remote areas and even directly from the aircraft, to enable rapid access to the image-derived information by the response community. Finally, the project to-date included successful testing and demonstration of the system on-site in Alaska, which included the participation of Alaska's Department of Environment, Alaska Clean Seas and US Coast Guard. In 2010 OI and OSPR received the US Department of Interior's Partners in Conservation Award for work conducted through this project.

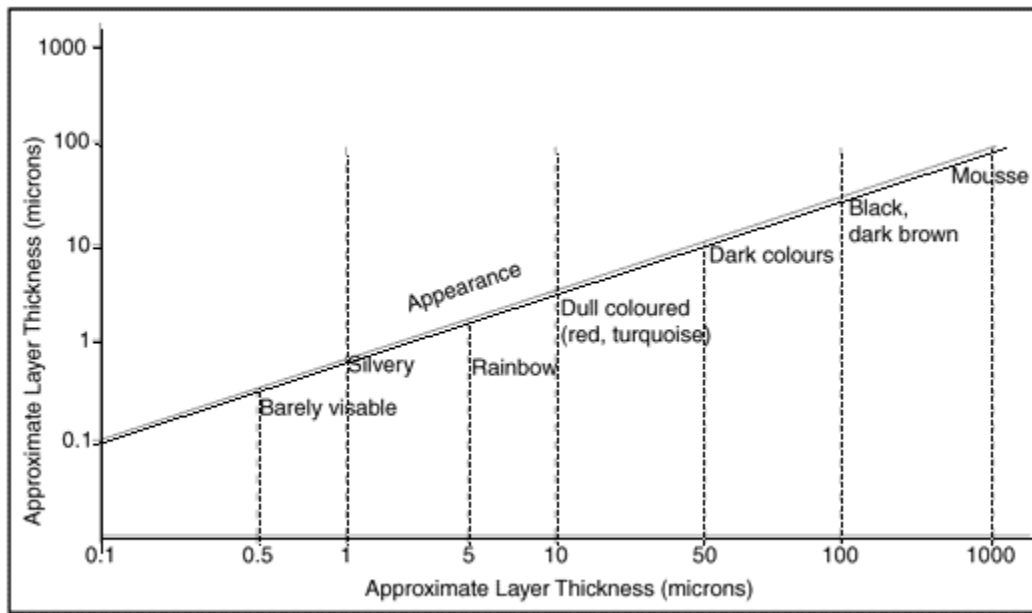
In early 2011 the project was extended to allow additional research and algorithm development specifically targeting oil emulsions. Heavily weathered and emulsified oil accumulations often constitute a large portion of recoverable oil in medium and large spills, and were commonplace throughout the Deepwater Horizon incident. The oil emulsion – oriented work consisted of utilizing archived multispectral and thermal imagery from the Deepwater Horizon spill to develop an initial algorithm, conducting controlled tests at Ohmsett to enhance the algorithm development, and conducting simultaneous aerial imaging and field sampling over naturally formed oil emulsion targets in the Santa Barbara Channel to use for the algorithm's validation. The development work centered utilizing readily available imaging technologies (CCD and microbolometer-based) rather than one-of-a-kind or experimental instruments which will likely not be readily available for operational use in future spills. The research determined that with such instrumentation the oil volume per unit of surface area within an emulsion film can be determined with good accuracy (rather than absolute film thickness which is not as clearly defined for emulsions as it is for fresh crude films). The resulting algorithm can thus separate oil emulsions from fresh oil, and map the spatial distribution of oil content within them – thus identifying areas with the largest oil volume for recovery, in-situ burning and dispersant application activities.

# 1. PROJECT BACKGROUND

## 1.1 Present-day Oil Spill Assessment Techniques

One of the most important initial steps in response to an oil spill at sea is the assessment of the extents of the oil slick and the quantity (i.e. thickness) distribution of oil within it. Since many types of hydrocarbons rapidly spread out to very thin layers when released at sea, accurate determination of which areas contain the most amount of oil is vital for efficiently guiding oil spill response efforts. Adages often mentioned by response crews such as “80% of the oil is contained in 20% of the slick” and “wasting time chasing sheens” illustrate the common, frustrating problem of misallocating time and resources due to insufficient knowledge of the oil thickness distribution within a spill.

The vast majority of oil quantity distribution assessments are presently done visually from helicopter or aircraft. Figure 1. shows thickness guidance parameters based on oil film appearance, which are commonly included in oil spill response training guides throughout the world. Such visual observations from aircraft (sometimes supplemented by drawings or digital photographs) suffer from three main complications. First, any verbal, graphic or oblique photographic documentation is usually based only on approximate geolocation information obtained through the aircraft’s GPS. Even if it is later reformatted as input into a computerized Geographical Information System (GIS), the data can contain a great degree of positional error. Second, visual estimation of oil film thickness distribution is highly subjective, is affected by varying light and background color conditions and, if not done by specially trained and experienced personnel, tends to be inaccurate. Most often the observers’ tendency is to overestimate the amount of oil present. Third, comprehensive visual assessments are impossible at night.



(Courtesy CONCAWE, A Field Guide to the application of dispersants to oil spills)

**Figure 1.** Oil-on-water appearance related to its thickness for guiding visual assessments. (From Gillot et al. 1988)

## 1.2 Project's Objectives and Approach

Our premise was to develop an aircraft or helicopter deployable system that would utilize the same universally tested and accepted spectral reflectance relationships between oil film thickness and its color appearance, but to eliminate the above-mentioned problems associated with visual observations by employing standardized multispectral camera systems for the imaging, and objective digital algorithms for the thickness estimation mapping. The addition of highly accurate geolocation devices to auto-georeference the imagery would also allow high location accuracy and the creation of a GIS-compatible, high resolution oil spill map product in near-real-time. An important consideration was to develop a system around relatively inexpensive, off-the-shelf hardware rather than a one-of-a-kind experimental or research-grade system that would have limited operational use.

OI utilized its own multispectral system – the DMSC MkII, manufactured by SpecTerra Ltd. in Australia. The imager provides 4 image channels, each at a customizable wavelength (using narrow band interference filters) between approximately 400 and 900nm. A 2-step algorithm approach was developed: a neural network-based algorithm is first applied to the data to create a binary oil/no-oil mask; a fuzzy ratio-based algorithm is then used on the oil-contaminated pixel areas to bin them into several thickness classes based on ratio relationships of the different wavelength channels compared to channel ratios of non-oiled areas (i.e. existing water background reflectance) (Svejkovsky and Muskat 2006, Svejkovsky et al. 2008). Previous work with thermal IR sensors done in Europe suggested the potential for IR imagers to have increased thickness detection capabilities for thicker oil films than is possible solely with imagery in the UV-visible-nearIR wavelength range (Byfield 1998, Davies et al. 1999). On the other hand, sheens and thin oil films tend to not be distinguishable in IR imagery. Our approach was therefore to combine the multispectral visible and IR systems and thus extend the measurable thickness range. This combined approach was found to provide good results and was utilized extensively during operational oil spill response support during the Deepwater Horizon incident.

The utilization of both visible and thermal wavelengths brings potential data processing complications specific to each wavelength type under different environmental conditions. For example, many ocean regions where oil is either drilled or transported are characterized by very turbid waters. While the thermal imagery can be expected to remain unaffected, reflectance from the suspended sediment will alter the background water reflectance characteristics in the visible wavelength channels and may thus also affect the developed oil identification and thickness estimation algorithms. Conversely, very cold air and/or water temperatures are not expected to alter oil and water reflectance characteristics in the visible channels but their potential effects on the water-to-oil thermal contrast parameters in the thermalIR imagery was heretofore unknown. One of this project's objectives was to investigate oil-on-water signatures under such conditions in order to allow more geographically universal, accurate utilization of the developed aerial mapping system. A related objective was to try to simplify the multi-camera, multi-wavelength system's hardware and technical operation requirements so that it could be operated by non-scientific personnel with minimal training.

The initial project plan focused on developing mapping capabilities for freshly spilled crude oils and IFOs. The common occurrence of emulsified oil during the extensive Deepwater Horizon oil spill underscored the need to extend the developed mapping capabilities to allow quantification of oil emulsions with aerial imaging systems, which had not been addressed to-date by the research community. The project was thus extended to allow the development of an oil emulsion-oriented algorithm. At this time, only two algorithms are known to exist that allow quantification of emulsified oil with aerial imaging: one developed and validated through this project, and one developed by Clark et al. (2010) using data collected over the Deepwater Horizon spill. An

important difference between the two approaches is that the Ocean Imaging algorithm utilizes image data from spectral ranges available through CCD (for multispectral imaging in the visible to short wave nearIR range) and microbolometer (for imaging in the thermal IR range), while the Clark et al. algorithm relies on long wave near-IR wavelength bands. Long wave nearIR imaging requires specialized imaging technologies that are not readily available and are thus less practical for implementing in an operational, relatively low-cost oil spill response system.

## **2. PROJECT RESULTS**

### **2.1 Task 1 - Determination & Initial Testing of Arctic Region-suitable Digital Dissemination System**

One of the perceived challenges of utilizing the aerial oil spill mapping system in Arctic regions (and other remote locations) is to be able to disseminate the digital images and image-based oil thickness maps to the response community in a timely manner. Cable or cellular internet links are relatively sparse and highly localized in Alaska and along the North Slope. OI therefore investigated a number of microwave and satellite-based transmission technologies that would enable the transmission of image data from remote locations.

Microwave systems offer by far the broadest bandwidth (i.e. fastest transmission speeds) and systems are available for both, land-based and in-the-air aircraft transmissions. All such systems are limited by essentially line-of-sight transmission to a ground receiving station that must be set up a priori. Hence, a ground-based receiver must be initially mobilized into the spill area before any data can be disseminated. This eliminates the possibility of utilizing the aerial oil mapping system as an initial, first-on-site spill survey method or its use early in the response. For this reason, OI primarily investigated satellite-based data transmission systems which are completely independent of ground support needs. Two such systems have been field tested to-date: 1) a Hughes 9201 BGAN Terminal which is a land-based (i.e. aircraft must land before data transmission) highly portable system with transmission speeds up to 492 Kbps. This terminal was successfully tested in the Anchorage, Alaska exercise (see below) and provides a practical data dissemination option. The unit retails for \$2750-\$4000, depending on battery capacity and other options; 2) a Thrane & Thrane Aviator 200 system which allows data (and voice) transmission directly from the aircraft. This system was tested during a Chevron-sponsored oil spill drill off San Diego in May, 2011. Analysis of its performance is attached in a de-brief in Appendix B.

The results of our tests indicate that with presently available technologies relevant for use with small aircraft, the most practical means to quickly disseminate data from the oil mapping system is to land the aircraft at a landing field where high speed cable or cellular wireless data links are available. In their absence, the BGAN terminal can provide a sufficient data link in remote regions. Relatively small amounts of data can potentially be effectively transmitted directly from the aircraft via the Aviator system.

### **2.2 Task 2 – Wintertime Testing of oil Thickness Mapping Sensor at Ohmsett**

As is mentioned above, the ability to utilize thermal imaging for oil spill mapping in Arctic or wintertime conditions had not been, to our knowledge, tested prior to this project. Petroleum substances have lower emissivity than water, and hence tend to “appear” cooler to an IR imager than surrounding water at the same temperature. This is true during both day and night for thin oil films composed of crude or refined petroleum substances. Thicker films composed of crude or other dark-colored petroleum mixtures trap solar heat during the day, however, and thus tend

to appear warmer than surrounding water under mild air and water temperatures. In order to assess the usefulness of thermal imaging for oil spill response in Arctic regions or in the winter months at higher latitudes, OI conducted experiments in BOEMRE's Ohmsett tank on 22-25 February, 2010. Following the previously established summertime experiment set-up, increasing volumes of several oil types were released in floating PVC pipe containment squares. The oil was spread throughout each square to create an adequately homogenous film whose thickness was known based on the total oil volume and square area. Oils tested included ANS, IFO380 and 20% and 60% emulsions created specifically for the experiments by Ohmsett engineers. Additional experiments were conducted without the containment squares, allowing the oil to spread out naturally and using plexiglass plates to sample oil thicknesses within various parts of the slick (see Svejkovsky and Muskat 2006 for methodology) Figure 2. shows the experimental setup. Since low water and air temperatures were not expected to appreciably affect algorithm results in the visible and near-IR portions of the spectrum, emphasis of the winter experiments was on thermal imaging. (The visible/near-IR imager would still be utilized, however, during operational, cold-weather use.) OI's thermal imager was mounted on the bridge's crow's nest above the test tank and the oil targets were sequentially imaged as the movable bridge traveled over them. Throughout the multi-day experiments air temperature varied between 38°F and 41°F and the tank's surface water temperature was between 36°F and 39°F. Heavy snow fell during the last day of the experiments.

The most important finding from the Ohmsett work was that the oil-to-water thermal contrast relationships established under summer conditions remain preserved even under near freezing temperatures: very thin oil films appear slightly cooler than water and thicker films appear warmer during the day. The heat retainment effect was evident even under heavily clouded skies and pertained to both crudes and emulsions. An interesting effect was observed when, prior to pouring the oil into the tank, the oil samples were first cooled to freezing by immersing the oil container in snow. Upon pouring the cooled oil into the tank, the oil film first appeared cooler than surrounding water, however, after 10-15 minutes the thicker portions of the slick reverted to appearing warmer – presumably by absorbing enough solar heat input during that period.

The Ohmsett work proved that thermal imaging can be utilized for oil spill mapping, and particularly for detecting the thickest portions of the spill, in Arctic or wintertime conditions using the same principles as were established for more temperate climates.



**Figure 2.** Crude oil samples being poured into floating containment squares in the Ohmsett tank (left) and sampling oil thickness in a patch of uncontained oil (right) during the wintertime experiments

### **2.3 Task 3 – Cold Environment IR Thickness Algorithm Development**

The data obtained at Ohmsett was used to refine the previously developed oil mapping algorithms. The oil-to-water thermal contrasts were similar to those observed under temperate conditions, however, for thick (>.5mm) oil films the contrast was smaller than expected using summertime data when, even under cloudy skies, thick oil films appeared up to 5°C warmer than the surrounding sea surface temperature. The thickness estimation relationship must thus be adjusted somewhat if estimates are being made over near-freezing waters.

Another important effect was observed during the Ohmsett tests that had to be remedied: the Jenoptik thermal imager includes internal calibration that is activated on a pre-set interval. Since image frames are potentially lost during the 2 seconds or so during the recalibration procedure, the process is usually done only every minute or less frequently. This is sufficient under moderate air temperatures, but during the Ohmsett work we found that the imager experiences very rapid calibration drift when the camera is exposed to near-freezing air temperatures (as it would be through an open port aboard an aircraft in the Arctic or in the winter). If uncorrected, the drift can cause major temperature inconsistencies after only 20-30 seconds of imaging, which in turn compromises proper and consistent oil thickness estimation from the entire imaging series. The condition necessitated that the thermal image acquisition software be altered to allow recalibration after every captured image frame (i.e. at usual aircraft speed of @ 100 knots, the system recalibrates itself approximately every 10 seconds). This modification alleviated the thermal drift problem.

### **2.4 Task 4 – Development of Simplified Multispectral System**

Throughout the development of the project's aerial oil mapping system OI utilized the SpecTerra DMSC-MkII multispectral sensor coupled with a Jenoptik thermal IR imager and Oxford Technologies DGPS/IMU unit. The Jenoptik and Oxford components are state-of-the-art, off-the-shelf available hardware that is also relatively well priced for its capabilities. The SpecTerra imager represents a more-or-less custom-made hardware/software combination (only 8 were manufactured, of which OI owns two). New units are no longer available, and the existing ones are based on non-current hardware and software technologies. One of the main goals of this project since its beginning was to design a portable, relatively low-cost and easy-to-operate system that could be purchased, operated and maintained by regional agencies or organizations. The availability of multiple, regionally-based systems is important in assuring that the equipment is readily available for immediate use near a future oil spill. Underscoring the interest in the potential for simplified, regionally based systems were inquiries to OI within the past 12 months from the State of Alaska (see next section) and the State of Washington. In the Washington case, the inquiry was part of newly enacted legislation that would mandate the mobilization of best available oil spill response technologies within 3 hours of the initial report of the spill.

As part of this project OI thus investigated available hardware/software options for efficient integration in a future aerial oil mapping system. We believe the Jenoptik and Oxford components represent high-quality, cost-effective units with good technical support and future upgrade capabilities. The DMSC multispectral component is more difficult to replace, because contemporary multispectral or hyperspectral imagers that have the needed oil-sensing capabilities are expensive (\$130,000 - \$500,000+), thus likely making the complete systems too costly for widespread ownership. OI was able to identify a promising technology, however, which provides the oil-sensing needs of multispectral (3-5 channels) through a single lens camera system. Its principle is a specially designed prism configuration which splits the incoming image into multiple components within the longUV-Visible-nearIR range, and redirects each subimage to a different CCD. The specific wavelength interval recorded by each CCD can be further narrowed

with narrow-band interference filters. OI investigated such prism systems from manufacturers in Italy and the Netherlands which offered 4-6 bands, but found them to have serious image quality deficiencies that preclude at this time their use in a multispectral oil sensing system. OI also tested a 3-band system from Japanese JAI Inc. and found that imager, while limited to three channels, to satisfy the image quality requirements for successful implementation of the developed oil mapping system when combined with a thermal IR imager. The JAI imager was tested over natural oil seeps in Santa Barbara Channel in October, 2012 and the first operational system is being assembled at this time. The approximate key hardware costs of the simplified system at the time of this writing are: Jenoptik thermal imager - @ \$36K, Oxford 2000 Series IMU - @ \$25K, JAI AT-200CL camera and ingestion card - @ \$7K. These components represent, by our tests, an adequate hardware configuration totaling less than \$100,000 with sufficient wavelength band combinations and geopositioning accuracy for effective oil spill mapping.

### **2.5 Task 5 – System Testing in Alaska.**

This project's original plan was to include a system test/demonstration exercise near Deadhorse, Alaska. Originally requested by Alaska Clean Seas, awareness of this project and its results grew, in part due to the developed system's widespread successful utilization during the Deepwater Horizon spill response. The exercise location was thus subsequently moved to Anchorage to allow more agencies to participate.

The exercise took place on 29 July, 2010. It was attended by representatives from the following agencies:

Cook Inlet Spill Prevention and Response, Inc. (CISPRI)  
US Coast Guard  
BOEMRE (Anchorage and Herndon offices)  
California Dept. of Fish & Game / Office of Spill Prevention and Response (OSPR)  
Alaska Fish & Wildlife Service  
Alaska Dept. of Environmental Conservation  
Alaska Clean Seas (North Slope office)  
Cook Inlet Regional Citizens Advisory Council  
British Petroleum (Alaska)  
Shell Oil  
NBC TV

In lieu of an actual oil slick target, fluoroscene dye was used as a proxy. The dye was released in a previously agreed-upon and permitted area in Cook Inlet by a CISPRI vessel which also carried some of the participants for on-the-water observations. Another smaller CISPRI vessel demonstrated the use of a containment boom as part of the exercise.

In-line with the project's objective that the developed aerial mapping system should be portable and mountable on local aircraft-of-opportunity, OI chartered a float-equipped Beaver aircraft from a local operator and mounted the system in the plane (installation took approximately 45 minutes). The plane then overflew and imaged the "oil slick" several times. Data processing was initiated while still airborne and completed upon landing and the resulting "oil spill" imagery and thickness map were disseminated via the portable BGAN transmitter (see Task 1 above) to a GIS server. OSPR's Judd Muskat, co-investigator in this project, was then able to immediately show and manipulate the map data with participants that remained in the "Command Center" set up in

BOEMRE's Anchorage office building. A full debrief and technology overview presentations were presented after the on-the-water participants returned to the "Command Center".

It should be noted that the Alaska exercise was conducted using OI's second DMSC imager, with the other continuing to be simultaneously deployed in the Gulf of Mexico as part of the Deepwater Horizon spill response. Overall, the exercise was met with enthusiasm from the various agencies who appreciated learning about the newly developed technology and seeing it deployed first-hand. A newspaper article summarizing the activity is attached here as Appendix A.

## **2.6 Task 6 – System Testing in Highly Turbid Waters (Gulf of Mexico)**

As was noted above, waters with large volumes of suspended sediments and/or plankton can be expected to be encountered in many regions with oil spill potential. The oil mapping algorithms, including multispectral imaging wavelength combination selections were developed from tank tests, and natural oil seep imaging studies with relatively clear underlying waters. This project therefore included a task to utilize naturally occurring seeps (or small oil well leaks) in the highly turbid region of the Mississippi River plume in the Gulf of Mexico. On 20 April, 2010 the Deepwater Horizon (DWH) oil rig exploded in the Gulf of Mexico and continued to spill oil into the sea until 15 July, 2010 when the wellhead was finally capped. Although the total amount of oil spilled remains under investigation, the spill is widely regarded as the second largest in history, exceeded only by the Mina al Ahmadi spill during the first Gulf War in 1991. Due to the size of the spill, traditional visual aerial surveys could not provide complete coverage of the spill area on a daily basis. As part of the response, multiple remote sensing technologies and sensors were mobilized. Under direction from the National Oceanographic and Atmospheric Administration (NOAA) and British Petroleum, OI was mobilized to aid the DWH Spill response on 1 May 2010. Following equipment installation on-board a NOAA Twin Otter aircraft, the oil mapping system was first utilized on 4 May 2010. In the following days, until 26 July 2010, the OI imaging and NOAA aircraft teams flew 1 to 2 imaging missions almost daily, based out of Mobile, Alabama.

Initially, most of OI's oil mapping activity focused on the spill source region and the spill seaward fringes, both being located in very clear water. In the ensuing weeks, however, as the oil began to reach nearshore, OI's missions began to also include areas around and in the Mississippi River Delta – the same locations with high suspended sediment loads that were to be targeted in the originally planned work. In conjunction with their operational mapping activities, OI staff was able to take advantage of the locations and aircraft availability to obtain and later analyze data suitable for this project. Large amounts of test imagery were acquired during plane transits over highly turbid areas that may not have been the prime targets of each mission but proved extremely useful for this project's analysis.

Figure 3. shows an example of relatively thick, emulsified oil over sediment-laden waters emanating from the Delta after a major rain storm.



**Figure 3.** Large patch of emulsified oil from the Deepwater Horizon spill floating on highly turbid Mississippi River effluent after a major rain storm.

OI's DWH response activities, oil mapping results and lessons-learned including the system's adaptations for turbid water conditions are subject of a soon-to-be-submitted manuscript to the peer-reviewed journal *Photogrammetric Engineering & Remote Sensing (PE&RS)*. For the purposes of this project progress report, we highlight the following findings:

High suspended sediment load in the water column tend to significantly decrease the background reflectance of the short-wavelength channels (i.e. non-oiled water appears darker in blue and green channels) and increase the background reflectance in longer visible wavelengths (i.e. yellow to red). Sediments also tend to increase reflectance in the near-IR (but not thermal IR) portions of the spectrum which tend to exhibit very low reflectance from clearer waters. Coincidentally, the high suspended sediment reflectances are also the reason why the use of nearIR wavelength channels for atmospheric attenuation corrections of satellite-derived chlorophyll imagery is compromised over coastal waters.

As applied to oil film sensing, the water-to-oil reflectance contrast is enhanced in short wavelength channels and even very thin sheens thus become more easily identifiable, as do thicker, darker oil accumulations. On the other hand, oil emulsions which tend to be highly reflective in the longer visible wavelengths and near-IR channels exhibit reflectances with lesser contrast to the water background than in clearer water regions. In addition, our research showed that red tides, which were prevalent in some of the Gulf areas, appear very similar to emulsified oil signatures in the near-IR bands.

These considerations lessen somewhat the value of near-IR channels for oil identification and mapping in highly turbid areas. It must be noted, however, that unemulsified, fresh crude oil signatures remain quite recognizable and characterizable using the developed methodologies. As is described below, subsequent research during this project specifically targeting oil emulsions showed that the thermal IR imagery is by far the most useful in quantifying oil emulsion properties. Since the thermal imagery is not significantly affected by high water turbidity, characterization of oil emulsions in high sediment load waters can still be successfully accomplished.

## **2.7 Task 7 - Determination of visible-nearIR and thermal IR response characteristics using imagery acquired during the Deepwater Horizon Oil Spill.**

The objective of this task was to utilize the multitude of image data acquired by OI during its 3-month support of the DWH spill response effort during summer 2010 to establish initial parameters related to oil emulsions' reflectance in the visible and nearIR portions of the spectrum, and thermal emittance in the thermal IR spectrum range. This research was to, in turn, guide further experiments at Ohmsett and the development of oil emulsion-specific algorithms that will allow estimation of oil/water content ratios and thickness patterns within floating emulsion accumulations.

Analysis of imagery showing obviously emulsified oil accumulations in the Gulf (as judged by the bright orange-red color of the oil and/or available field data) immediately refuted a contention that has been repeatedly quoted in scientific literature – that oil emulsions are generally not detectable with thermal IR imagers because their water content causes them to have heat emittance characteristics very similar to the surrounding water. To the contrary, emulsified oil features tended to exhibit strong thermal contrast relative to surrounding water, with its variability apparently linked to the emulsion's thickness and likely also oil/water ratio. (Our results did support other previously published reports that oil sheens and very thin films are not distinguishable in thermal imagery.) Figure 4 shows an example from OI's DWH-acquired imagery. While providing operational oil map products during the DWH response, OI utilized its previously developed oil thickness algorithms to create maps of oil concentrations in areas of fresh, unemulsified oil but, not having algorithms for emulsions, classified all emulsified oil targets into a single "emulsion" class. Our initial analyses under Task 7 indicated that a more detailed characterization of the various emulsion states is possible utilizing the visible-nearIR multispectral data in conjunction with thermal imaging.

The initial analyses focused on better understanding of relationships between the visible-nearIR reflectances and thermal IR emittance characteristics. The initial analyses guided experiment design and multispectral channel wavelength selection for experiments planned at BOEMRE's Ohmsett facility in October, 2011. The quantitative, controlled experiments were an important step in advancing the research of validated oil emulsion classification algorithm since no field samples of oil emulsions simultaneously collected with the DWH imagery have been available to OI for image data calibration and algorithm development. However, while at Ohmsett (see Task section 2.9) OI staff met with scientists from Canada's SL Ross who did collect numerous field samples of DWH emulsions in areas often imaged by the OI system. Although none of the SL Ross samples perfectly coincided with the locations of imagery collected on the same day by OI, several were within the general vicinity and did provide useful field-based documentation.

The initial DWH data analyses resulted in the following guidelines for development of an oil emulsion quantification algorithm:

- 1) Emulsions exhibit high reflectance in the near-IR wavelength range – in contrast to fresh crude oil which exhibits very low reflectance.

- 2) The reflectance variability of oil emulsions in various wavelength bands within the visible range is not distinctly related to the films thickness and/or oil-to-water content ratio.
- 3) Known oil emulsion targets imaged by OI during DWH with the thermal IR sensor exhibit distinct signals that vary with thickness and likely their oil-to-water content ratio.

The initial algorithm development approach thus focused on first utilizing the sensor's near-IR band to identify emulsified oil targets and separate them from fresh oil, then utilize the thermal imagery to quantify the film's content. Because of the lack of adequate amount of reliable field sampling data from DWH to help establish the quantification parameters, however, it was deemed necessary to conduct detailed, controlled experiments at Ohmsett before the quantification aspects of the algorithm could be adequately addressed.

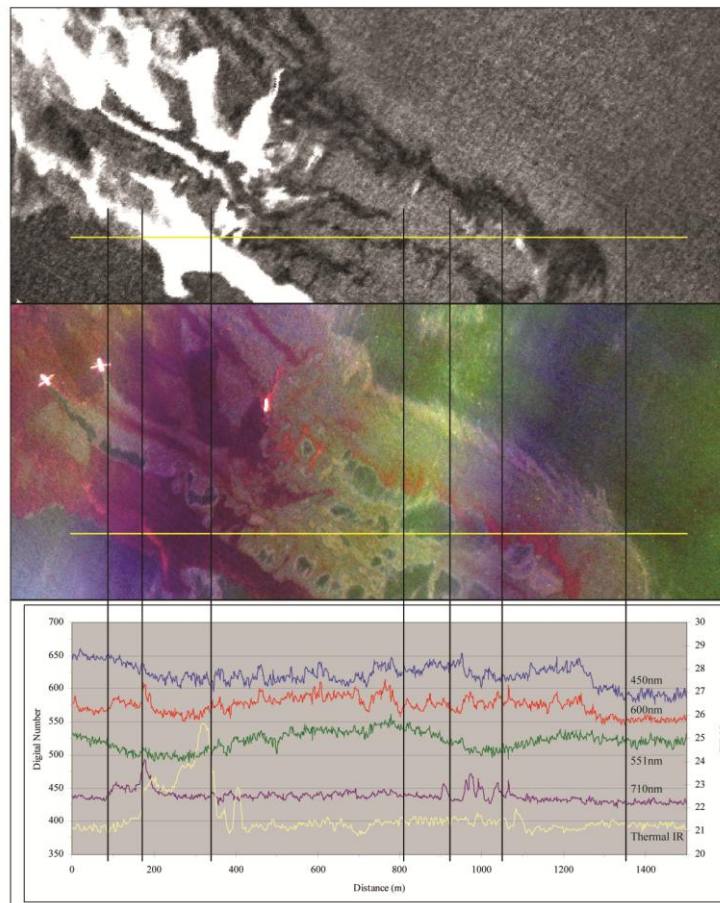


**Figure 4.** Thermal IR (top) and 450, 551 and 600nm color rendition of a large area of emulsified oil during the DWH spill as imaged by Ocean Imaging's aerial system. The graphs on the bottom show spectral reflectance/emission profiles along the yellow transect line. The thickest emulsions show the highest heat emission (white areas in top image) while thinner emulsions appear cooler (darker) than surrounding water due to petroleum's lower emissivity properties. (from Svejksky et al. 2012)

## **2.8 Task 8 - Initial oil emulsion characterization algorithm development.**

This task was originally scheduled for completion before the data acquisition and testing work at Ohmsett in October, 2011 (Task 9). However, as is stated above, upon initial analysis of data acquired during the DWH spill, the initial oil emulsion quantification algorithm approaches required additional data from the Ohmsett tests to provide sufficient background for defining quantification relationships between the sensed thermal contrast and the emulsions' composition. Hence, we completed Task 8 after including results obtained at Ohmsett.

An important factor related to oil emulsions and any multispectral algorithm development for their quantification was established during the analysis of data from DWH, other oil emulsion data obtained in earlier projects over natural oil seeps, and Ohmsett experiments with laboratory created emulsions: Crude oil emulsions created under controlled conditions in the laboratory do not exhibit drastically different reflectance properties (relative to fresh crude) in the visible through short and mid nearIR (up to 1000nm) regions of the spectrum (although their reflectance does increase in the red to nearIR with increasing water/oil content ratio). In contrast, naturally formed emulsions as observed during DWH, other spill events, and near oil seeps typically exhibit an orange to red color and greatly increased reflectance in the nearIR. Additionally, field-collected bright emulsion samples collected during DWH by S. L. Ross Ltd. rapidly lost their orange or red hues when placed in a glass collection jar (R. Belore pers. communication, Belore et al. 2011). The origin of the typical bright color of naturally formed emulsions is unclear and is being further investigated in this project. It is not due to asphaltenes or other compounds as claimed by Clark et al. (2010) because such compounds are also present in the various types of crudes from which emulsions were created at Ohmsett and would thus have shown similar effects. More likely, it may be the result of combined effects of the accumulation through time of organic materials as the emulsion floats around the sea surface, the oil's weathering and UV-caused breakdown, and other factors. As evidenced by S. L. Ross' analysis of the DWH field samples, differences in color appearance of emulsions do not consistently exhibit the same differences in water/oil ratios and thicknesses. This difference between reflectance properties in the visible-nearIR region of natural and laboratory-created oil emulsions has been largely unknown and/or ignored by other researchers attempting to develop multispectral image-based methodologies for the quantification of oil spills. For this reason, our initial emulsion characterization algorithm development focused on using the visible-nearIR wavelength channels only for general identification of emulsified vs. unemulsified oil (primarily due to significant reflectance differences in the near-IR region), and then attempting to extract quantitative characteristics of the emulsions from the thermal IR channel. Combined analysis of DWH imagery and controlled experiments at Ohmsett confirmed that at thicknesses typically encountered with emulsified oil slicks, the emulsions exhibit (in daytime) significant thermal contrasts relative to the surrounding sea surface temperature (SST). At a particular slick thickness, however, the thermal contrast is significantly lower than is observed for an unemulsified, fresh crude

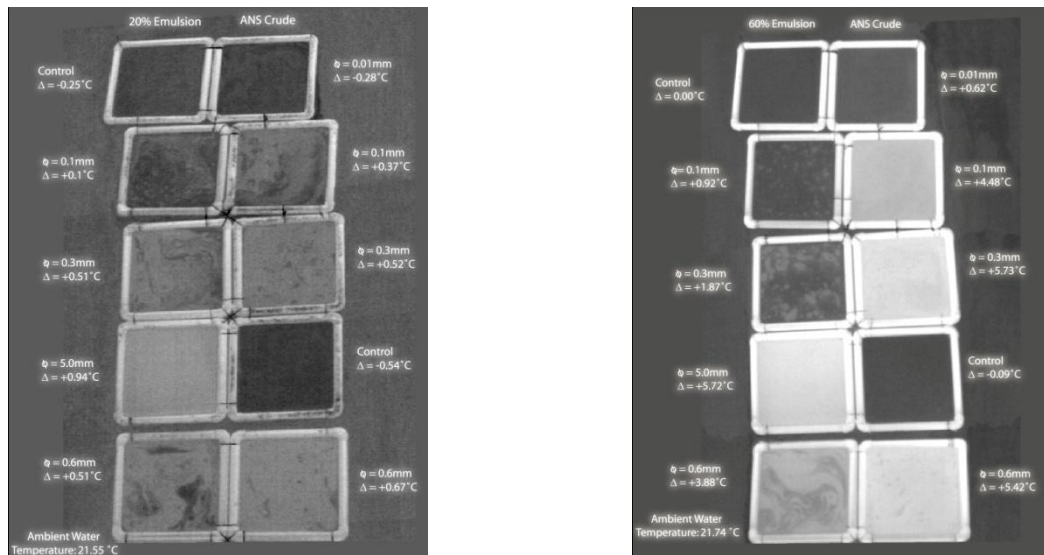


**Figure 5.** Sample thermal imaging data sets from Ohmsett experiments. On the left are shown containment squares with differently thick films of 20% (water) emulsions and pure ANS crude, as imaged under cloudy conditions. On the right is the same set-up using 60% (water) emulsion but imaged under sunny skies.

film under the same SST, air temperature and wind conditions. This difference increases dramatically as the water content of the emulsion increases under both sunny (high solar heat input) and cloudy (lower solar heat input) sky conditions. An example of this effect is shown with Ohmsett data in Figure 5.

As could be expected, both water/oil ratio and thickness of the emulsion film independently alter the detected thermal contrast. However, at thicknesses greater than approximately 1mm the thermal contrast increase (relative to surrounding SST) becomes asymptotic and is much more dependent on the emulsion's oil content than on actual thickness of the oil/water/air mixture. This is a fortunate property for 2 reasons: 1) Knowledge of the water/oil ratio is a very important parameter for the successful application of dispersants or in-situ burning; 2) Unlike fresh crude films which have well defined upper and lower boundaries, emulsion films (especially older ones) tend to have an uneven, sponge-like lower boundary – making the determination of exact thickness somewhat relative. Also, as was evidenced in field samples during DWH, some emulsion accumulations can reach thicknesses of several centimeters, making it impossible to passively determine their true thickness from surface reflectance or thermal emission characteristics. We thus intend to primarily concentrate on the accurate determination of the water/oil ratio in characterizing emulsion films.

## 2.9 Task 9 – Controlled oil emulsion data acquisition and initial approach testing at Ohmsett

OI staff and project collaborator Mr. Judd Muskat from CDFG OSPR visited Ohmsett the week of 9 October, 2011. There were two prime objectives of the Ohmsett activities: 1) to conduct imaging experiments on emulsions with known oil/water ratios and film thickness compositions; 2) to explore further under controlled conditions observations made during DWH imaging which indicated that thermal imaging may be useful for

documenting the effects of aerial dispersant applications on both emulsified and unemulsified oil.

As in previous Ohmsett experiments, PVC pipe squares were floated in the Ohmsett tank to act as containment barriers into which known quantities of oil emulsions were poured and spread. This created emulsion films of known thicknesses. Two representative emulsion compositions, created by Ohmsett staff, were used: 20% water and 60% water contents. Unemulsified Alaska North Slope (ANS) crude oil was also used for reference. OI's multispectral and thermal IR camera systems were mounted on the tank's movable bridge's crows nest and the oil-containing squares were imaged as the bridge moved over them. Because the tank's bottom is painted white and its depth is only @ 8', bottom reflectance is not typical of a natural ocean's deep water spill. Hence, as we have done in the past, a blue-green canvas tarp was placed on the tank's bottom below the test squares to more closely approximate deep water reflectance characteristics in the visible wavelength range (nearIR and thermal IR do not appreciably penetrate the water column and bottom reflectance is thus not an issue). The tank also was experiencing a green algae bloom during the tests which may have biased the visible wavelength spectra toward the green more than usual.

Figure 6 shows the imaging square targets. Several initial results can be noted in this interim report: First, during the day the thermal contrast between the 60% emulsions and surrounding water is considerably smaller (approximately a factor of 10) for a given film thickness than pure crude oil. This is logical in that the water-containing oil emulsion absorbs and re-emits less solar heating than pure crude. The relationship is consistent with smaller oil/water content ratios (i.e. the 20% emulsion samples had IR emittance closer to pure oil) and is an important aspect considered in the emulsion-oriented classification algorithm presently under development. Second, as was already noted above from the initial DWH emulsion data analysis, even relatively thin emulsions can be readily detected in IR imaging, although their daytime thermal signature makes them appear cooler than the surrounding water, a reversal relationship also observed with pure crude films. Hence a combination of thermal and vis-nearIR imaging is important in distinguishing oil emulsions from unemulsified oil, and for characterizations of the emulsions' properties.

On one of the Ohmsett days, the experiments were continued into nighttime to document changes in the oil and oil emulsion signatures when solar heat input ceases to affect the oil films. As was expected, both oil types reverted to appearing cooler than surrounding water after sundown, but important differences in the thermal contrast related to emulsified water content were observed.

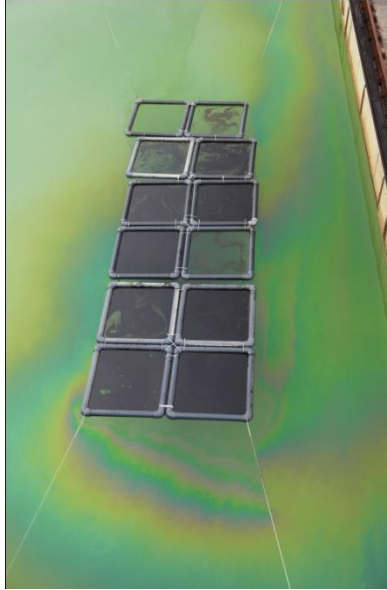


**Figure 6.** Floating PVC squares containing various thickness films of pure ANS crude oil emulsions and no oil for control purposes. Following each imaging experiment the squares were emptied of oil with a water jet and refilled with oil and emulsions of different thickness and oil/water ratios.

On the last day of the Ohmsett experiments, the dispersant application objective was addressed. Because of the high interest from the oil industry and dispersant research community in this subject, we have prepared a web-page presentation of the initial data and results discussion. The material can be accessed at:

<http://www.oceani.com/DispersantExperiment> is now protected. The page is password protected:

User name: OIDispTest

Password: OI246oil

The initial results supported OI's observations during DWH that suggest thermal aerial imaging could provide a very useful broad-area coverage dispersant effectiveness documentation technique that could be added to the existing (ship-based) SMART monitoring protocols.

### **2.10 Task 10 - Advanced Algorithm Development**

The objective of this task was to build upon initially derived oil emulsion principles in the visible-nearIR-thermal IR spectrum bands and develop an operationally useful emulsion characterization algorithm that would provide useful quantification of emulsified oil distributions during a spill. As is discussed in the previous progress report under Task 8, initial algorithm development work showed that upon identifying a floating oil target as emulsified using multiple visible-nearIR wavelength bands, the measurement of its thermal contrast relative to the surrounding water provides the most reliable means to quantify its oil content.

Additional work under Task 10 confirmed that, unlike in the case of unemulsified oil films that tend to have both their upper and lower boundaries well defined, the absolute

thickness of emulsions, especially older, weathered emulsions, is not so clearly defined. Often the lower (i.e. submerged) boundary consists of a sponge-like texture, with water and air pockets interspersed between vertical strands of oil.

As could be expected, both water/oil ratio and thickness of the emulsion film independently alter the detected thermal contrast. However, at thicknesses greater than approximately 1mm the thermal contrast increase (relative to surrounding SST) becomes asymptotic and is much more dependent on the emulsion's water/oil content ratio than on actual thickness. Based on advanced analysis of data obtained at Ohmsett in October, 2011 and another Ohmsett visit in December, 2011 funded by ExxonMobil as part of a separate (dispersant-testing) project, as well as further analysis of data from DWH and Santa Barbara oil seeps, the final emulsion quantification algorithm provides a measure of actual oil content per unit of surface area, rather than an estimation of the film's "thickness". We believe that a reliable estimate of the actual oil volume within the emulsion is of the most relevance to recovery and other response operations rather than a (as per our tests unreliable) estimate of a "thickness" which does not reflect the actual oil/water content ratio.

The final algorithm development work also addressed the effects of clear versus cloudy sky conditions, based on test data obtained at Ohmsett. The thermal contrast decreases significantly, although predictably, when imagery is obtained under a heavy cloud layer (in one case during a light drizzle). An adjustment for existing solar irradiance is thus part of the algorithm. The final emulsion-quantification algorithm is incorporated into OI's previously developed oil mapping classification flow: First, a neural network-based step is used to isolate all oil-containing pixels (both unemulsified and emulsified) from oil-free water pixels and non-oil artifacts; second, based on high/low reflectance characteristics in the available visible and near-IR bands, unemulsified and emulsified oil areas are separated; third, non-emulsified oil pixels are binned into thickness classes using a fuzzy ratio algorithm (Svejkovsky et al. 2008); fourth, residual, emulsion-containing pixels are classified using separate look-up tables relating thermal contrast between surrounding SST and the oil containing pixel to oil volume contained in a unit surface area of the emulsion film.

### **2.11 Task 11 - Emulsion Mapping System Tests Over Santa Barbara Oil Seeps**

The objective of this final task was to simultaneously collect aerial imagery and field samples from actual emulsified oil targets in the Santa Barbara Channel, California, created by natural oil seeps. The data sets were then to be used for validation of the developed emulsion-oriented quantification algorithm. This work was originally planned for summer, 2012 utilizing an aircraft made available to the project at no cost by CDFG-OSPR. Plane availability and weather-related problems prevented the tests to be done as originally planned, and Ocean Imaging requested and was granted a time-extension of the project to allow this task to be completed in the fall of 2012.

The aerial and field sampling was successfully done on 9 and 10 October, 2012. On both days suitably large targets of emulsified oil exhibiting a variety of color reflectance and

thermal emittance properties were located from the aircraft and their locations communicated to a 33' sampling vessel. When on-site, the vessel was then further verbally guided by marine radio into an exact sampling position and the entire region was imaged with OI's aerial system several times while samples of the emulsions were collected from the vessel. The oil-to-water ratio of each sample was determined by weighing the initial emulsion samples, and subsequently separating the oil/water volumes by heating each sample following the procedures of Clark et al. 2010 and Belore et al. 2011. 16 different samples from 8 sample sites were acquired for analysis. 4 samples were deemed incompletely oil/water separated and/or contaminated during sampling, leaving 12 valid samples for the algorithm evaluation. Figures 7 - 9 show examples of the sampling vessel in position, an emulsion target being sampled, and an aerial thermal image of the sampling site.

Figure 10 shows the results of the algorithm validations. The imaging-based emulsion oil quantifications show significant agreement with the actual field measurements. The sources of error affecting the correlation include not only those related to the algorithm's computation but also in the difficulties of sampling from a wave-moving platform, and errors inherent in the heating-derived separation of the oil in each sample. Additionally, it must be noted that the relative thicknesses and hence volumes of emulsions encountered in the Santa Barbara Channel were somewhat small when compared to some emulsion accumulations found during DWH and sampled and documented by, for example SL Ross. Nevertheless, our results show that emulsion compositions can be quantified with a CCD/microbolometer-based aerial imaging sensor and, in our opinion, can provide useful and valuable information on oil distributions for more effective response.



**Figure 7.** Sampling vessel approaching one of the selected oil emulsion targets on 10/10/2012. Care was taken to drift into the emulsion rather than use the boat's motor which could disturb the oil film.



**Figure 8.** Oil emulsion patch being sampled.

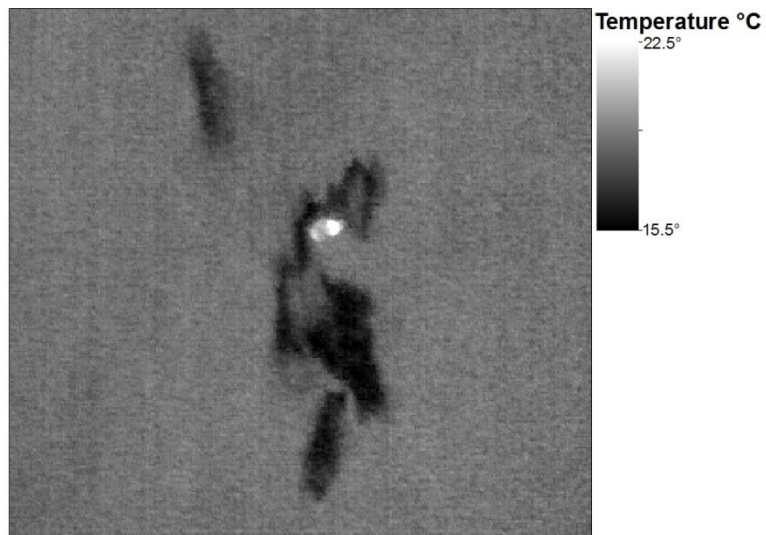


**Figure 9.** Thermal signature of the emulsion patch seen in Figure 2 as imaged with Ocean Imaging's aerial system. The sampling vessel appears white (warm).

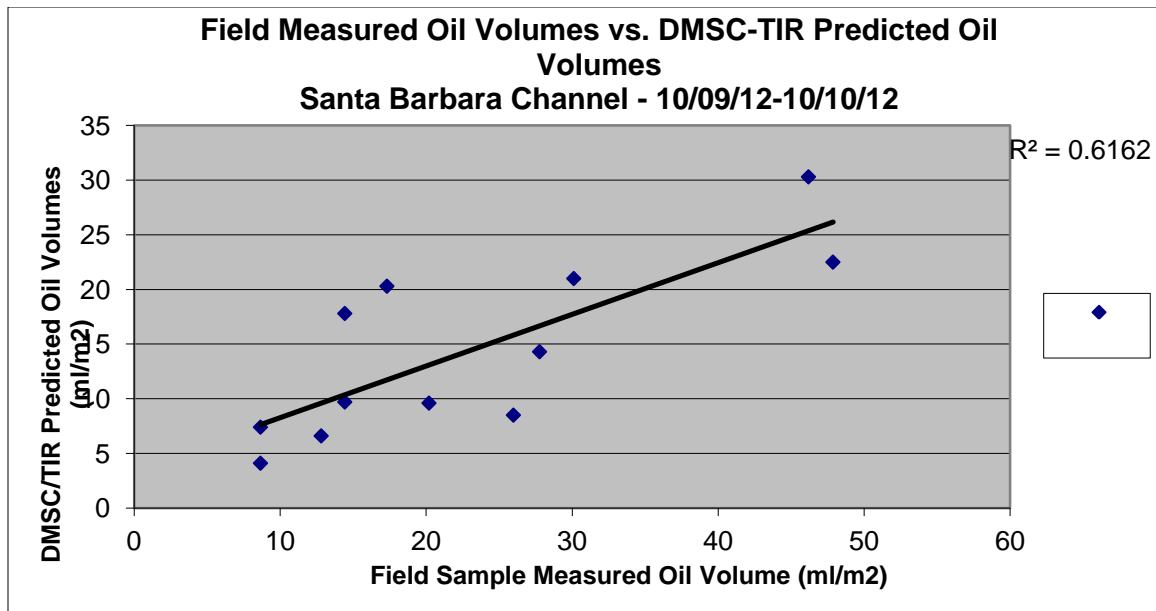


**Figure 10.** Comparison of aerial image-derived and field measured oil quantities from samples collected from emulsion targets in the Santa Barbara Channel 9-10 October, 2012.

### 3. PUBLICATION OF RESULTS

One of the proposed deliverables of this project was the publication of results in a peer-reviewed scientific journal. The Deepwater Horizon oil spill which occurred during this project's timeline, and OI's operational utilization of the developed oil mapping algorithms during the spill response provide an opportunity not only to publish the project's main results but to also report on their utility as well as limitations as applied in an actual large-scale oil spill. Following internal reviews by NOAA and BSEE (the paper has co-authors from both agencies), and journal-managed peer-review, the resulting paper has been published in the October, 2012 issue of *Photogrammetric Engineering and Remote Sensing*:

Svejkovsky J., W. Lehr, J. Muskat, G. Graettinger and J. Mullin. 2012. **Operational utilization of aerial remote sensing during oil spill response: Lessons learned during the Deepwater Horizon spill.** *Photogrammetric Engineering and Remote Sensing*, Vol. 78 (10), 1089-1102.

The paper is attached as Appendix C.

The latest emulsion-related results obtained in the final months of this project will also be included in a future publication detailing thermal IR imaging technologies as applied to oil spills.

### 4. REFERENCES

Belore, R. C., K. Trudel, J. Morrison. 2011. Weathering, Emulsification, and Chemical Dispersibility of Mississippi Canyon 252 Crude Oil: Field and Laboratory Studies. *Proceedings of the International Oil Spill Conference 2011*, 23-26 May, Portland, Oregon, unpaginated USB flash drive.

Byfield, V. 1998. Optical Remote Sensing of Oil in the Marine Environment. PhD Thesis, U. of Southampton, School of Ocean and Earth Science.

Clark, R. N., G. A. Swayze, I. Leifer, K. E. Livo, R. Kokaly, T. Hoefen, S. Lundeen, M. Eastwood, R. O. Green, N. Pearson, C. Sarture, I. McCubbin, D. Roberts, E. Bradley, D. Steele, T. Ryan, R. Dominguez, and the Airborne Visible/Infrared Imaging Spectrometer (AVIRIS) Team, 2010. *A Method for Quantitative Mapping of Thick Oil Spills Using Imaging Spectroscopy*. USGS Open-File Report, 2010-1167, 51 p.

Davies L., J. Corps, T. Lunel and K. Dooley. 1999. Estimation of oil thickness. AEA Technology. AEAT-5279(1). 1-34.

Gillot, A., G.H.R. Aston, P. Bonanzinga, Y. le Gal la Salle, M.J. Mason, M.J. O'Neill, J.K. Rudd and D.I. Stonor. 1988. Field guide to application of dispersants to oil spills. Rept No.2/88. The Hague, Netherlands, CONCAWE. 64pp.

Svejkovsky, J. and J. Muskat. 2006. Real-time detection of oil slick thickness patterns with a portable multispectral sensor. Minerals Management Service, Final Report for Project #0105CT39144.

Svejkovsky, J. 2007. Development and evaluation of a cost effective aerial imaging system for oil spill and coastal impact monitoring. Final Report to Calif. Dept. of Fish and Game's Office of Oil spill Prevention and Response, Contract #P0375037.

Svejkovsky, J. 2008. Determination and testing of wavelength combination options for imaging oil-on-water with a UAV. Final Report to Navy-SPAWAR Systems Center, Contract #N66001-08-M-1080

Svejkovsky J., J. Muskat and J. Mullin. 2008. Mapping Oil Spill Thickness with a Portable Multispectral Aerial Imager. Proc. International Oil Spill Conference 2008, 4-8 May, 2008, Savannah, Georgia.

## 5. APPENDIX A

### News article from the Arctic Sounder

#### New technology could aid oil spill workers

Published in [the Arctic Sounder](#) By Victoria Barber  
Aug 5th, 2010



Crewmembers aboard the Guardian spray two gallons of neon yellow dye into the Cook Inlet as part of an oil spill mapping exercise. (Alaska Newspapers, Victoria Barber)

ANCHORAGE - State, federal and industry representatives got to glimpse the changing face of oil spill response last week.

On July 29, about 20 observers boarded the fishing vessel Guardian. Normally the boat would be hauling crab pots on the Bering Sea, but that day it was dumping gallons of neon yellow liquid into the Cook Inlet. Overhead a plane made several passes as three boats equipped with boom and skimmer stood at the ready.

The yellow fluid, a biodegradable dye, was being poured by crewmembers into the inlet to demonstrate a new system that could change the way the industry responds to oil spills. Working under contract with the U.S. Bureau of Ocean Energy Management Regulation and Enforcement,

a California-based company has created the new system to help skimmer crews target their oil spill recovery.

This system was launched just this year and includes several devices - an aerial multispectral camera, which takes images at four different wavelengths, an infrared camera and a differential GPS unit. It is portable and can be mounted into a camera port of a small plane. The unit used during the demonstration is one of only two units currently in existence.

The cameras and sensors in the system look for one thing - not so much where the oil is, but how thick it is.

"There's an adage in oil spill recovery - you don't want to chase sheen," said Jan Svejkovsky, president of Ocean Imaging, the company that developed the equipment.

When oil gets into the ocean it creates a thin slick that floats on the surface, most of it a rainbow- or silver-colored sheen. Sheens look dramatic, but they are also misleading, Svejkovsky said.

"You see the sheens and say - 'oh my god look at all this oil.' But it's all sheens potentially and you don't know where the thick stuff is," Svejkovsky said.

Sheens can't be burned, skimmed or boomed. Furthermore, sheen doesn't contain very much oil. When crews with skimmers respond to a spill, they look for thick, brown or black globs of crude, because that's the oil they can clean up.

Oil disperses quickly once it's released, so timing is crucial. Crews have to get to the oil before it dissipates into the ocean if they are going to capture it. To find thick oil crews usually rely on aerial observers, who are trained to tell the difference between concentrated oil and sheens. This new system essentially replaces that observer with a computer, taking out the element of human error and speeding up the process by transmitting digital maps to a server in real time as it's flying over the site.

After the tour of the inlet, Svejkovsky projected the multispectral camera's picture of the yellow dye "spill" onto a screen in an Anchorage boardroom. In the image, the ocean looks like a violet field, with a long yellow stain trailing behind the dark spot of the Guardian. The image was sent to the boardroom while Svejkovsky was still in flight that morning. Once people on land had the image they could overlay it with details like shipping routes, coastal features or other information, Svejkovsky said.

But what the picture didn't show was the capability that's probably most exciting for Alaska - its view of the world in infrared.

Just as a regular camera takes pictures of light and color, an infrared camera can take pictures of temperature. Oil heats and cools at a different rate than water, so the infrared camera can tell where the oil concentrations are based on the temperature difference. For infrared imaging, it doesn't matter if it's dark outside. That's important in Alaska, where it's dark much of the year.

Joseph Mullin manages the oil spill response research program under the Bureau of Ocean Energy Management, Regulation, and Enforcement (BOEMRE). He coordinated the demonstration because he thinks it's important for agencies like the Coast Guard, oil spill

response companies and state agencies to get on board with improved technologies - before they need it.

"The right time to try new technology is not in an emergency," Mullin said.

That's not how it worked out in the Gulf of Mexico. Svejksky's company was planning a test run in the Gulf when the Deepwater Horizon drilling rig exploded, leading to a massive oil spill. Svejksky has been working with NOAA on mapping the spill using the new technology system since May 1.

The fact that it's already being used in the Gulf spill will probably go a long way in promoting its adoption in Alaska, said Bob Mattson, manager of the Prevention and Emergency Response Program in the Alaska Department of Environment.

The problem with oil spill technology is that operators can't dump real oil into an ocean to try the equipment out, and trace dyes or water tank conditions don't perfectly mimic a real world spill.

"One of the few silver linings in a spill is the ability to test new technology like this," Mattson said.

The system has application beyond an accidental spill. Similar technology is currently being used in Europe to help police boats illegally offloading fuel into the ocean.

Mattson said the demonstration had convinced him of the usefulness of the device, but it remained to be seen which branch of government or corporation would cough up the \$100,000 to \$150,000 for the equipment.

"The devil's in the details," Mattson said.

## 6. APPENDIX B

### Debrief of Data Transmission Systems tested during Chevron Oil Drill

**Activity Synopsis:** On both days all work was done close to originally formulated time-line. California Dept. of Fish & Game's Partenavia aircraft (F&G 8) arrived on-station over MSRC's *M/V California Responder* shortly after 10am. Radio communication was established with both the Responder and the USAF C-130 en-route to the "oil spill" location. F&G8 instructed the Responder to begin releasing the oil-proxy dye. Upon completion, with some dye left unreleased for Ocean Imaging's (OI's) work later, a reflective marker buoy was dropped into the thickest portion of the dye, in the effort to provide a visual marker for the C-130 crew. F&G8 then proceeded to act as a spotter and guide for the C-130 "dispersant" water spraying over the dye. Multiple passes were successfully done with good accuracy. Upon completion of the aerial spray exercises, F&G8 instructed the Responder to release whatever dye was left for the aerial imaging tests. The dye remained visible considerably longer on 5/11 than on 5/12 but could be adequately imaged on both days. The release constituted of a relatively thin line of dye which quickly separated from the vessel. OI crew aboard F&G8 imaged the dye with their multispectral sensor and the image and ancillary data were sent to OI's Denver office for processing via the Thrane & Thrane Aviator 200 aerial satellite system. On both days the data were successfully transferred and immediately processed for "oil thickness", then disseminated to the response community in a variety of file formats. OI also arranged to test a marine data dissemination system aboard the Responder – the Sailor 250 – and successfully sent the "oil spill" analysis maps directly to the vessel, as well as was able to stay in touch with the vessel crew via e-mail.

**Test Equipment Overview:** The two systems tested represent state-of-the-art equipment that retails for relatively low (<\$100K) costs and is suitable for small aircraft and vessels to transfer digital data between each other at speeds faster than the rudimentary data transmission rates presently available on such wide-spread satellite-based systems as Iridium and GlobalStar. In OI's view, a satellite-based system (versus microwave or HF) is the most logical solution for data transmission during an oil spill response because it requires no ground station set-up and support. While much higher data transfer speeds are possible with the alternate systems, the need for a ground station receiver precludes the system's use as a first-on-site system, in remote areas, or far offshore.

The Thrane & Thrane Aviator 200 system is presently the only "low cost" (@ \$40-50K) hardware set-up for small aircraft. It is not entirely portable because a small, fin-shaped antenna must be mounted on top of the aircraft, but the rest of the hardware can be readily moved and connected from one plane to another. As its name implies, the system claims capability of data transfer rates up to 200 Kbps. The boat-mounted Sailor 250 system is part of a line of marine-oriented systems spanning a range from 150 to 500 Kbps. Hardware cost for the Sailor 250 is @ \$9-10K. Both systems incur data transfer costs during use ranging from \$9 to \$13 per Megabyte of data transferred, depending on usage plan.

**Testing Results and Practical Considerations for Oil Spill Response:** Both systems performed satisfactorily. An apparently malfunctioning GPS antenna on the aerial system may have compromised the system's performance somewhat during the first testing day.

**Aerial system testing:** OI's DMSC-MkII 4-channel aerial multispectral imager outputs 4-banded, 12-bit, 1024x1024 pixel image frames which are just slightly over 8 Megabytes in size. In practical operation, frames are acquired as the aircraft flies over the oil spill, with some frame-

to-frame overlap (usually 40-60%) to allow for proper mosaicking of the data. The area coverage of each frame depends on the aircraft altitude. At 12,500 feet (maximum practical flying altitude without passenger oxygen requirements in an unpressurized aircraft) the frame footprint is approximately 2km<sup>2</sup>, with spatial resolution of approximately 2m. OI's Jenoptik thermal imager has similar imaging geometry but (due to its microbolometer technology) lower spatial resolution. When compressed with lossless algorithms, each DMSC frame is approximately half its initial size – i.e. @ 4MB.

On-ground and in-air tests of the Aviator 200 system resulted in DMSC data transfer rates of approximately 8MB in 5.75-7 minutes. This equates to approximately one uncompressed or two compressed DMSC frames being transferred every 6 minutes. This performance rate should be put into perspective of a real oil spill: OI's imaging of the Dubai Star spill in San Francisco Bay consisted of one line of 6 image frames to cover the spill area. Similar DMSC imaging of the Platform A spill in the Santa Barbara Channel required 3 overlapping lines of imaging, each containing 10-14 frames. (Flight altitude was chosen to adequately resolve needed spatial detail in each spill). Coverage of the central region of the Cosco Busan spill in San Francisco Bay on the third day of the spill required approximately 120 frames. During OI's work on the Deepwater Horizon spill in the Gulf of Mexico, hundreds of frames from both the DMSC and thermal imagers were acquired and processed each day.

The data transfer rate achieved with the Aviator 200 system thus does not appear to be sufficient to be practically useful for multispectral data transfer during medium or large oil spills, since the time needed to transfer the data can be the same or longer than it would take for the aircraft to fly back to a nearby airport and offload the data using a standard LAN or wireless network.

However, the system would be quite useful for the following applications: 1) transmission of thermal-only imagery whose files are much smaller than the multispectral DMSC files and are immediately useful for identifying the thickest oil areas; 2) transmission of ancillary images such as oblique photos in JPEG or similar (lossy) compression formats for immediate, qualitative documentation of the spill; 3) data transfer over spills in very remote areas where the nearest internet-connected landing site is far away or not logistically reachable (it should be noted that according to Thrane & Thrane's service coverage map, Alaska's North Slope does NOT have system coverage).

**Vessel-at-sea system testing:** The Sailor 250 system performed quite well on board the Responder. Using ancillary software, the crew was even able to send video to the Response Command showing the progress of the dye discharge during the exercise. From a practical, operational standpoint an oil response vessel on-site likely does not have the same high-volume image data dissemination needs as the remote sensing aircraft. Hence, the tested system appears quite adequate and could be highly useful in a real response situation.

**Operational Cost Considerations:** As was noted above, data transfer charges for both, the aerial and marine systems are approximately \$11 per Megabyte. Hence, the air-to-ground transfer of raw data image sets equivalent to those acquired over the Dubai Star and Platform A spills would cost several hundred to \$1000+ each. On the other hand, the shore-to-ship transfer of final oil spill map products (in the form of PDFs, GoogleEarth or other GIS compatible files) would be relatively inexpensive. It should be noted that alternate (boat-mounted, not aircraft-compatible) satellite-based data transmission systems (e.g. VSAT) will likely become available in the near-future, providing similar or better transfer capabilities but at significantly lower transmission costs (ostensibly as low as \$0.50 per MB).

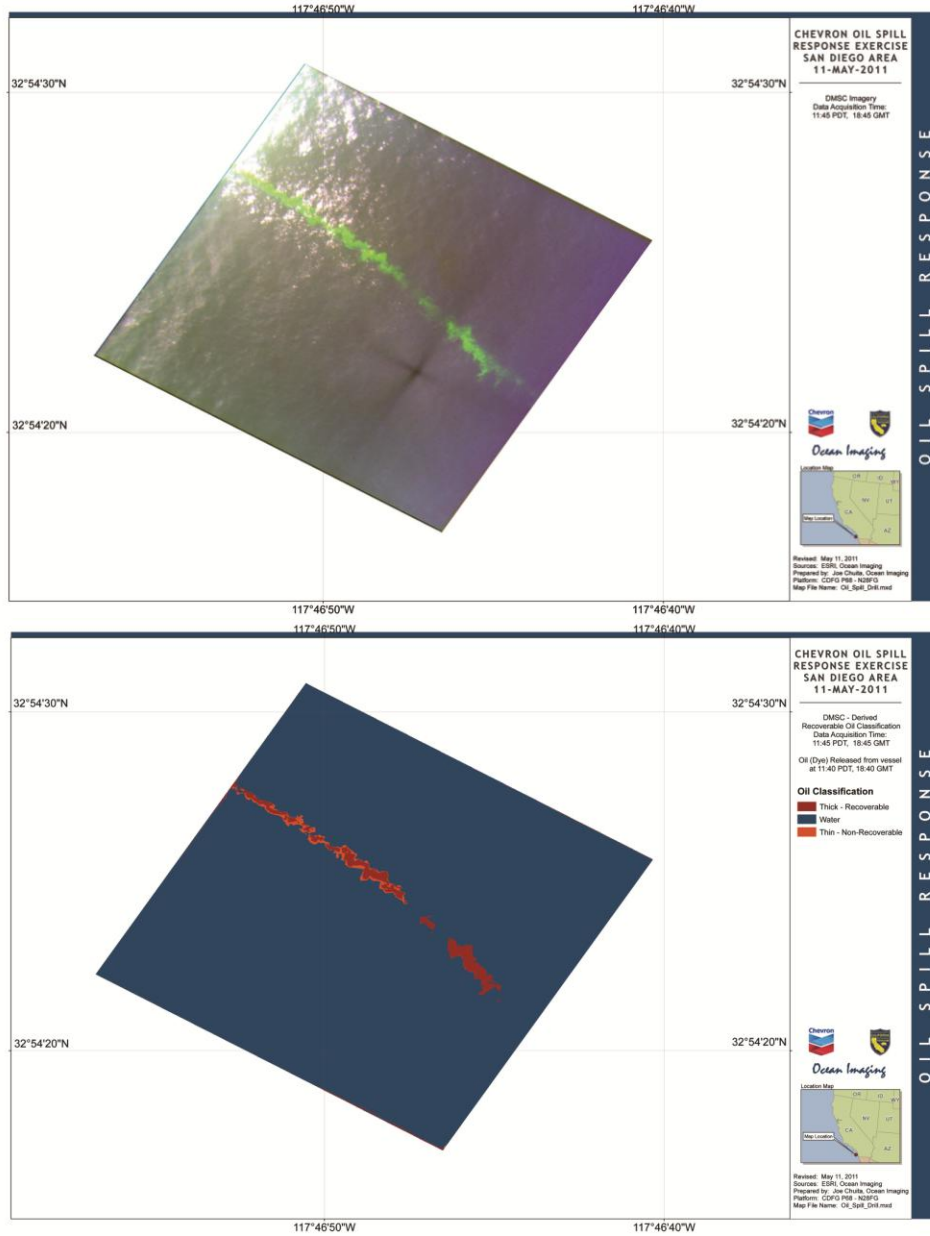
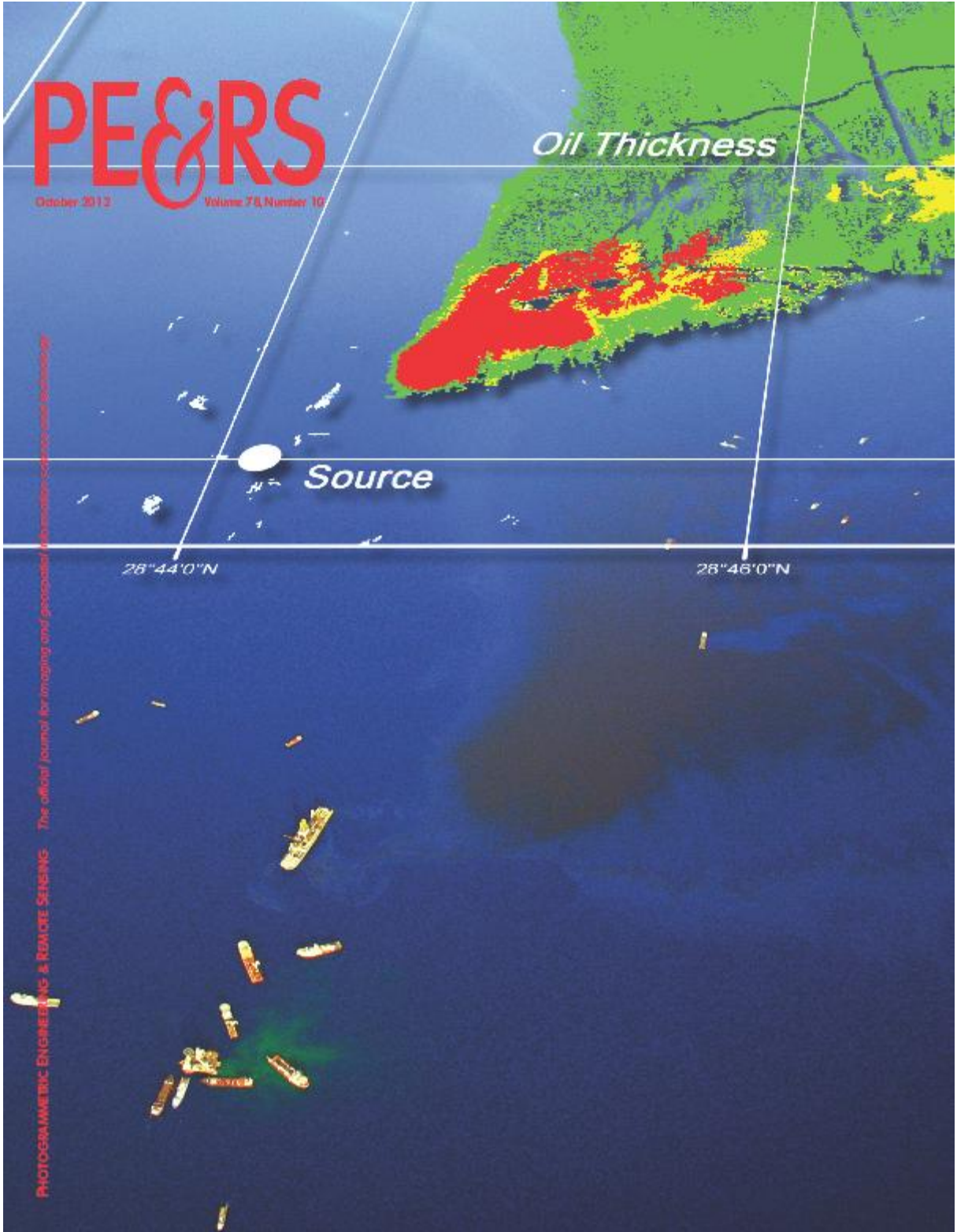


**Figure 1.** DMSC multispectral image of the oil-proxy dye on 5/11/2010 (top) and resulting “oil thickness” classification product that was transmitted to the M/V California Responder

7. APPENDIX C



## This image composite shows an aerial photo of the region around

the source site of the Deepwater Horizon (MC-252) oil spill in the Gulf of Mexico on 5/26/2010. Overlaid is an oil thickness distribution map derived from Ocean Imaging Corp.'s aerial multi-spectral mapping system. The system's oil thickness derivation algorithm used three channels in the visible, one in the near-IR and one in the thermal-IR to assign the oil-containing pixels into several thickness classes. Such GIS-compatible maps of the source region and other regions of priority within the spill were generated once to twice daily and electronically disseminated to the response community. More details on the imaging and how it was utilized throughout the response can be found in a peer-reviewed article in this issue. The surface oil signature is displaced from the actual bottom source location due to currents that affected the oil as it took 4+ hours to rise from the 1500m depth. The greenish feature between the vessels in the lower left corresponds to residual drilling mud used during one of several different attempts to inject material into and plug the leaking well. For more information on the system and Ocean Imaging Corp. see [www.oceani.com](http://www.oceani.com) or call 858-792-8529. Cover image art by Paula Klein, Ocean Imaging.



## Highlight Article

### 1011 Expanding the Utility of Remote Sensing Data for Oil Spill Response

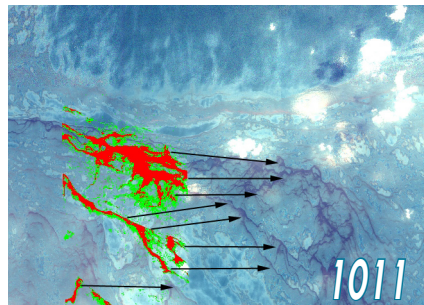
Jan Svejtkovsky and Mark Hess

## Columns & Updates

### 1015 Grids and Datums – Maps in the Middle of Nowhere

### 1017 Book Review – *Remote Sensing and Global Environmental Change, First Edition*

### 1020 Industry News

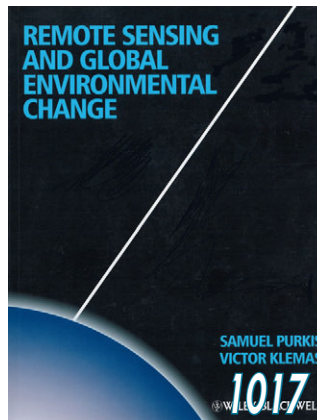


## Announcements

### 1005 New from ASPRS – *Manual of Airborne Topographic Lidar*

### 1023 ASPRS 2013 Annual Conference – *Confluence by the Bay – A Gathering of Geospatial Insights*

### 1068 Call for Papers – *Geospatial Responses to Disasters: A Holistic Approach (Web-based GIS/Mobile Devices)*



## Departments

### 1019 New Members

### 1019 Classifieds

### 1021 Member Champions

### 1022 Certification List

### 1024 Who's Who in ASPRS

### 1025 Sustaining Members

### 1027 Instructions for Authors

### 1078 Forthcoming Articles

### 1088 Calendar

### 1103 Advertiser Index

### 1103 Professional Directory

### 1104 Membership Application

# PE&RS

October 2012

Volume 78, Number 10

PHOTOGRAMMETRIC ENGINEERING & REMOTE SENSING  
The official journal for imaging and geospatial information science and technology

## JOURNAL STAFF

### Publisher

James R. Plasker  
[jplasker@asprs.org](mailto:jplasker@asprs.org)

### Editor

Russell G. Congalton  
[russ.congalton@unh.edu](mailto:russ.congalton@unh.edu)

### Executive Editor

Kimberly A. Tilley  
[kimt@asprs.org](mailto:kimt@asprs.org)

### Technical Editor

Michael S. Renslow  
[renslow76@comcast.net](mailto:renslow76@comcast.net)

### Assistant Editor

Jie Shan  
[jshan@ecn.purdue.edu](mailto:jshan@ecn.purdue.edu)

### Assistant Director – Publications

Rae Kelley  
[rkelley@asprs.org](mailto:rkelley@asprs.org)

### Publications Production Assistant

Matthew Austin  
[maustin@asprs.org](mailto:maustin@asprs.org)

### Manuscript Coordinator

Jeanie Congalton  
[jcongalton@asprs.org](mailto:jcongalton@asprs.org)

### Circulation Manager

Sokhan Hing  
[sokhanh@asprs.org](mailto:sokhanh@asprs.org)

### Advertising Sales Representative

The Townsend Group, Inc.  
[asprs@townsend-group.com](mailto:asprs@townsend-group.com)

## CONTRIBUTING EDITORS

### Grids & Datums Column

Clifford J. Mugnier  
[cjmce@isu.edu](mailto:cjmce@isu.edu)

### Book Reviews

John Iames  
[liames.john@epamail.epa.gov](mailto:liames.john@epamail.epa.gov)

### Mapping Matters Column

Qassim Abdullah  
[Mapping\\_Matters@asprs.org](mailto:Mapping_Matters@asprs.org)

### Website

[webmaster@asprs.org](mailto:webmaster@asprs.org)



Immediate electronic access to all peer-reviewed articles in this issue is available to ASPRS members at [www.asprs.org](http://www.asprs.org). Just log in to the ASPRS web site with your membership ID and password and download the articles you need.

## Peer-Reviewed Articles

### 1029 A Supervised and Fuzzy-based Approach to Determine Optimal Multi-resolution Image Segmentation Parameters

Hengjian Tong, Travis Maxwell, Yun Zhang, and Vivek Dey

A novel technique to effectively determine optimal image segmentation parameters for eCognition and improve the segmentation efficiency and accuracy.

### 1045 Automated Georegistration of High-Resolution Satellite Imagery using a RPC Model with Airborne Lidar Information

Jaehong Oh, Changno Lee, Yangdam Eo, and James Bethel

A new method for automated georegistration of high-resolution satellite imagery using a RPC model with existing airborne lidar data.

### 1057 Generation of a U.S. National Urban Land-Use Product

James A. Falcone and Collin G. Homer

A proposed method and examples for building a national urban land-use grid representing thematically-detailed classes.

### 1069 A Flexible Mathematical Method for Camera Calibration in Digital Aerial Photogrammetry

Rongfu Tang, Dieter Fritsch, Michael Cramer, and Werner Schneider

A new family of rigorous and flexible self-calibration additional parameters (APs) and strategies for assessing the full potential of in-situ camera calibration.

### 1079 Mapping Individual Tree Species in an Urban Forest Using Airborne Lidar Data and Hyperspectral Imagery

Caiyun Zhang and Fang Qiu

A neural network based classifier to identify individual tree species by integrating lidar data and hyperspectral imagery.

### 1089 Operational Utilization of Aerial Multispectral Remote Sensing during Oil Spill Response: Lessons Learned During the Deepwater Horizon (MC-252) Spill

Jan Svejkovsky, William Lehr, Judd Muskat, George Graettinger, and Joseph Mullin

Oil slick spatial extent and thickness estimation maps derived from a multispectral visible, near-IR and thermal IR aerial imaging system were successfully utilized for multiple applications during the Deepwater Horizon oil spill.

**PHOTOGRAMMETRIC ENGINEERING & REMOTE SENSING** is the official journal of the American Society for Photogrammetry and Remote Sensing. It is devoted to the exchange of ideas and information about the applications of photogrammetry, remote sensing, and geographic information systems.

The technical activities of the Society are conducted through the following Technical Divisions: Geographic Information Systems, Photogrammetric Applications, Primary Data Acquisition, Professional Practice, and Remote Sensing Applications. Additional information on the functioning of the Technical Divisions and the Society can be found in the Yearbook issue of *PE&RS*.

Correspondence relating to all business and editorial matters pertaining to this and other Society publications should be directed to the American Society for Photogrammetry and Remote Sensing, 5410 Grosvenor Lane, Suite 210, Bethesda, Maryland 20814-2144, including inquiries, memberships, subscriptions, changes in address, manuscripts for publication, advertising, back issues, and publications. The telephone number of the Society Headquarters is 301-493-0290; the fax number is 301-493-0208; email address is [asprs@asprs.org](mailto:asprs@asprs.org).

**PE&RS.** *PE&RS* (ISSN0099-1112) is published monthly by the American Society for Photogrammetry and Remote Sensing, 5410 Grosvenor Lane, Suite 210, Bethesda, Maryland 20814-2144. Periodicals postage paid at Bethesda, Maryland and at additional mailing offices.

**SUBSCRIPTION.** Effective January 1, 2012, the Subscription Rate for non-members per calendar year (companies, libraries) is \$420 (USA); \$436 for **Canada Airmail** (includes **5% for Canada's Goods and Service Tax** (GST#135123065)); \$430 for all other foreign.

**POSTMASTER.** Send address changes to *PE&RS*, ASPRS Headquarters, 5410 Grosvenor Lane, Suite 210, Bethesda, Maryland 20814-2144. CDN CPM # (40020812)

**MEMBERSHIP.** Membership is open to any person actively engaged in the practice of photogrammetry, photointerpretation, remote sensing and geographic information systems; or who by means of education or profession is interested in the application or development of these arts and sciences. Membership is for one year, with renewal based on the anniversary date of the month joined. Membership Dues include a 12-month subscription to *PE&RS* valued at \$68. Subscription is part of membership benefits and cannot be deducted from annual dues. Annual dues for Regular members (Active Member) is \$135; for Student members it is \$45 (E-Journal – No hard copy); for Associate Members it is \$90 (see description on application in the back of this Journal). An additional postage surcharge is applied to all International memberships: Add \$40 for **Canada Airmail**, and 5% for **Canada's Goods and Service Tax** (GST #135123065); all other foreign add \$60.00.

**COPYRIGHT 2012.** Copyright by the American Society for Photogrammetry and Remote Sensing. Reproduction of this issue or any part thereof (except short quotations for use in preparing technical and scientific papers) may be made only after obtaining the specific approval of the Managing Editor. The Society is not responsible for any statements made or opinions expressed in technical papers, advertisements, or other portions of this publication. Printed in the United States of America.

**PERMISSION TO PHOTOCOPY.** The appearance of the code at the bottom of the first page of an article in this journal indicates the copyright owner's consent that copies of the article may be made for personal or internal use or for the personal or internal use of specific clients. This consent is given on the condition, however, that the copier pay the stated per copy fee of \$3.00 through the Copyright Clearance Center, Inc., 222 Rosewood Drive, Danvers, Massachusetts 01923, for copying beyond that permitted by Sections 107 or 108 of the U.S. Copyright Law. This consent does not extend to other kinds of copying, such as copying for general distribution, for advertising or promotional purposes, for creating new collective works, or for resale.

---

Is your contact information current?

Contact us at [members@asprs.org](mailto:members@asprs.org)

or log on to <http://www.asprs.org/Member-Area/>  
to update your information.

We value your membership.

---

# Operational Utilization of Aerial Multispectral Remote Sensing during Oil Spill Response: Lessons Learned During the Deepwater Horizon (MC-252) Spill

Jan Svejkovsky, William Lehr, Judd Muskat, George Graettinger, and Joseph Mullin

### Abstract

*A rapidly deployable aerial multispectral sensor utilizing four channels in the visible-near-IR and one channel in the thermal IR was developed along with processing software to identify oil-on-water and map its spatial extents and thickness distribution patterns. Following validation over natural oil seeps and at Bureau of Safety and Environmental Enforcement's (BSEE's) Ohmsett test tank, the system was utilized operationally on a near-daily basis for three months during the Deepwater Horizon (MC-252) spill in the Gulf of Mexico in summer 2010. Digital, GIS-compatible analyses were produced and disseminated following each flight mission. The analysis products were utilized for a multitude of response activities including daily offshore oil recovery planning, oil trajectory modeling, dispersant application effect documentation, beached oil mapping and documentation of the relative oil amount along the spill's offshore perimeter. The system's prime limitation was its relatively narrow imaging footprint and low sun angle requirement to minimize sunglint, both of which limited the total area that could be imaged each day. This paper discusses the system's various applications as well as limitations that were encountered during its use in the Deepwater Horizon incident.*

### Introduction

Rapid determination of the spatial extents of an oil slick during and after an at-sea spill is vital for evaluating response needs, and initiating and guiding spill response

---

Jan Svejkovsky is with Ocean Imaging Corporation, 201 Lomas Santa Fe Dr., Suite 370, Solana Beach, CA 92075 (jan@oceani.com).

William Lehr and George Graettinger are with the National Oceanographic and Atmospheric Administration, 7600 Sand Point Way NE, Seattle, WA 98115.

Judd Muskat is with the California Department of Fish & Game, Office of Spill Prevention and Response, 1700 "K" Street, Sacramento, CA 95811.

Joseph Mullin is with Joseph Mullin Consulting, LLC, 8003 Chestnut Grove Road, Frederick, MD 21701. (Retired from Bureau of Ocean Energy Management, Regulation, and Enforcement after this research was conducted).

activities. Just as importantly, oil thickness distributions are beneficial for proper choice of response methods and spatial allocation of response resources. However, accurate oil film thickness/volume estimation remains a difficult challenge (Lehr, 2010; Brown *et al.*, 2005).

The major remote sensing technique for oil spills is visual observations and recordings by a trained observer. Various formulas have been built to link slick appearance with spill thickness. The earliest reported system in the literature was a 1930 report to the US Congress that listed six thickness categories from 0.04  $\mu\text{m}$  to 2  $\mu\text{m}$ . A more widely circulated standard, done by American Petroleum Institute in 1963, closely followed this earlier report. Hornstein (1972) developed a standard that was based upon actual experiments; under controlled laboratory lighting, he spilled known quantities of different crude and refined oils into dishes, then documented their appearances. This standard is still widely used in response guidebooks. It divides oil thickness into five groups ranging from 0.15  $\mu\text{m}$  to 3.0  $\mu\text{m}$ . The European response community has produced its own set of standards, the most widely disseminated being those connected with the Bonn Agreement (Bonn Agreement, 2007). The Bonn Agreement Aerial Surveillance Handbook (BAASH) uses an appearance code based upon previously published scientific papers, small-scale laboratory experiments, mesoscale outdoor experiments and field trials. The visual, appearance-based methodology suffers from three main complications, however. First, any verbal, graphic, or oblique photographic documentation is usually based only on approximate geo-location information obtained through the aircraft's Global Positioning System (GPS). Even if it is later reformatted as input into a computerized Geographical Information System (GIS), the data can contain a great degree of positional error. Second, visual estimation of oil film thickness distribution is highly subjective and, if not done by specially trained and experienced personnel, tends to be inaccurate. Most often the observers' tendency is to overestimate the amount of oil present, resulting in the recovery crews' losing valuable time

---

Photogrammetric Engineering & Remote Sensing  
Vol. 78, No. 10, October 2012, pp. 1089–1102.

0099-1112/12/7810-1089/\$3.00/0  
© 2012 American Society for Photogrammetry  
and Remote Sensing

“chasing sheens” rather than concentrating on the thicker accumulations. Third, comprehensive visual assessments are impossible at night.

Aerial and satellite imaging can, in principle, provide a convenient means to detect and precisely map marine oil spills, and provide timely information for guiding recovery operations. Advances in imaging technologies within the last two decades have increased the utilization of aerial imaging in oil spill detection and response, and side-looking airborne radar (SLAR) and ultraviolet/infrared (UV/IR) detectors are being used operationally in Europe (Zielinski, 2003; Trieschmann *et al.*, 2003; Brown and Fingas, 2005). Europe’s oil pollution recognition programs are nationally or multi-nationally funded with a fleet of dedicated aircraft equipped with specialized oil-sensing instruments (Bonn Agreement, 2007). No such program of similar magnitude presently exists in the United States. In most cases, observer aircraft are provided by the responsible party, US Coast Guard or a regional/state spill response agency.

On 20 April 2010 the Deepwater Horizon (DWH) oil rig exploded in the Gulf of Mexico and continued to spill oil into the sea until 15 July, 2010 when the wellhead was finally capped. Although the total amount of oil spilled remains under investigation, the spill is widely regarded as the second largest in history, exceeded only by the Mina al Ahmadi spill during the first Gulf War in 1991 (NOAA, 2011). Due to the size of the spill, traditional visual aerial surveys could not provide complete coverage of the spill area on a daily basis. As part of the response, multiple remote sensing technologies and sensors were mobilized. The most frequently utilized data during the response were provided by Synthetic Aperture Radar (SAR) sensors aboard Canadian Radarsat satellites, Moderate Resolution Imaging Spectroradiometer (MODIS) instruments aboard National Aeronautics and Space Administration’s (NASA’s) Aqua and Terra satellites, aerial Side-Looking Airborne Radars (SLARS) flown by Transport Canada and Icelandic Coast Guard, and multispectral visible and thermal infrared imagery flown by USA’s Ocean Imaging Corporation (OI). (Several other imagers, both federal and corporate, collected data primarily for research, test, or baseline documentation purposes but were not deployed on a routine, daily basis and did not provide the imagery for daily response activities.) The volume of remote sensing data collected from these sources and their daily application during the lengthy spill represents to-date the most intense utilization of remote sensing technologies during an oil spill incident. It was also the first instance when maps of oil spill distribution and thickness derived from aerial multispectral visible-near-IR and thermal IR imagery were operationally produced and widely disseminated during various facets of the response effort. This paper focuses on the utilization of the acquired aerial multispectral imaging for the different response activities, how this imaging technology was integrated with the other remote sensing resources, and the major lessons learned from applying the aerial remote sensing technology in such a large-magnitude event.

## Background and Methodology

The detection of oil spills has been demonstrated with both aerial and satellite-based instruments. Numerous technology review articles have been published that discuss the various remote sensing approaches and their limitations (e.g., Fingas and Brown, 1997; Brekke and Solberg, 2005; Jha *et al.*, 2008; Lehr, 2010; Fingas and Brown, 2011). For the purposes of this paper the following paragraphs briefly summarize the most commonly recognized instruments with emphasis on their practical, operational application.

The most commonly utilized satellite and aerial sensors are SARs, which detect oil by its surface slick signature. The presence of a surfactant film on the water surface suppresses capillary waves and thus reduces the backscatter return intensity over the slick area. The effect can also be observed with passive instruments such as MODIS when the satellite imagery contains sunglint off the ocean surface (Hu *et al.*, 2009). Present SAR technology is not readily able to distinguish between true oil signatures and biogenic slicks or low-wind affects, however, and is thus sometime subject to a high incidence of false targets. SAR imaging is also not able to quantify oil thickness, rendering even the thinnest (and unrecoverable) sheens the same or very similar as thick oil and oil-emulsion accumulations whose locations are of prime interest for efficient spill response. On the other hand, both satellite and aerial SARs can provide relatively wide spatial coverage, making them very useful (as was the case in the DWH spill) for assessing the total extents of surface oil and their changes in time during a large spill. Additionally, the unique ability of these instruments to penetrate cloud cover and be effective at night allows them to provide updated information with consistent frequency.

Another instrument type that has been tested for oil slick detection and some thickness measurement is the laser fluorosensor. The instrument uses a downward-looking laser to excite fluorescence in floating oil molecules, and detects the fluorescence-caused backradiation in the ultraviolet UV part of the spectrum. Since the instrument is dependent on the excitation effects of its laser, however, the aircraft carrying it must fly very close to the ocean surface (maximum altitude is usually 150 to 180 meters, up to 600 meters for high-powered XeCl excimer laser systems). The result is a thin line of data corresponding to the laser’s track along the aircraft’s flight path. A recently developed scanning laser fluorosensor extends the line of measurements into an “image” path up to 200 meters wide (Brown and Fingas, 2003). The high cost and one-of-a-kind nature of that instrument greatly restricts its operational use. Although laser fluorometry is quite effective at detecting oil on the ocean, the need for extensive criss-cross flying to map even a medium-size spill as well as the obvious possible dangers of flying at such a low altitude under adverse wind conditions limit its operational use. Additionally, under real-world conditions, the Raman signal used for thickness determination with laser fluorometry tends to disappear over films thicker than approximately 10  $\mu\text{m}$  (Lennon *et al.*, 2006), with the signal’s suppression limiting detection and thickness estimation to films in the range of 0.1  $\mu\text{m}$  to 10  $\mu\text{m}$  (Hengstermann and Reuter, 1990; Goodman and Brown, 2005). To our knowledge, laser fluorometry has not yet been successfully utilized for operational support during an actual oil spill.

UV-sensing imagers detect petroleum’s high reflectance in the UV band. This effect occurs even over very thin oil sheens, and UV sensors are thus useful for oil detection and surveillance purposes. As with SAR imaging, however, (although due to different physical properties) the technology provides almost no information on oil thickness, making it of limited use for actual oil spill response where it is important to distinguish the locations of thicker oil accumulations from the usually much larger sheen areas.

As was already mentioned, thermal imaging has shown promise in oil spill mapping. A number of past studies have shown that thermal IR sensors have the potential to identify the thicker oil films (Byfield, 1998) and can be used to direct skimmers to thicker portions of the slick (Fingas and Brown, 1997). One IR-based system utilizing a neural network approach to classify oil slick thicknesses into a number of thickness classes claimed to reach accuracies

of 76 to 82 percent for oil films up to several millimeters thick when a range of sea state and atmospheric parameters were known (Davies *et al.*, 1999). A thermal imager also makes it possible to continue mapping and monitoring the oil spill during nighttime. As previous studies and OI's own research have shown, however, an oil spill mapping effort based solely on IR imagery can be quite complex: oil sheens generally cannot be identified, but thin films may appear cooler than the surrounding water during both day and night, due at least in part to petroleum substances' lower than water emissivity properties. Thicker (and hence darker) crude oil films tend to trap and re-emit solar heat input and thus appear warmer than water during the day. After sundown they revert to appearing cooler due to the emissivity difference.

Visual assessment of oil-on-water thickness is based on optical properties within the visible wavelength range that change with increasing oil thickness. The utilization of a multispectral imaging system configured to maximize the same optical properties can thus represent a potentially more effective extension of the traditional visual oil spill surveys. The visible wavelength range can be further augmented by cameras that image in the near-IR and thermal IR. The vast recent advancements in vis-near-IR multispectral and thermal IR camera technologies provide such systems with significant potential for becoming useful operational tools during oil spill response efforts. With emphasis on developing an easy-to-deploy, operationally useful oil spill mapping system, OI has conducted research since 2004 on oil identification and thickness classification algorithms using a multispectral system in the visible-near-IR-thermal IR wavelength range. The objective was to apply the same general principles of the existing visual oil classification parameters, augmented by near-IR and thermal-IR bands, to drive software that objectively classifies the image pixels into oil thickness classes based on their individual spectral characteristics. In addition to outputting a high resolution, accurately located GIS-compatible map of the oil features, the system should reduce the subjectivity inherent in visual observations made by multiple observers on different days. The emphasis was on operational-oriented image acquisition and processing using portable, relatively inexpensive acquisition and processing hardware that could be quickly mounted in an aircraft-of-opportunity, operated by minimal personnel and produce quantitative map products in near-real-time. For these reasons, a multispectral (a few channels) rather than a hyperspectral (a dozen to 100+ channels) system was used. However, advances in both hyperspectral data cube processing techniques (Boggs and Gomez, 2001), and imaging hardware may render hyperspectral technology practical in such future real-time or near-real-time oil spill mapping systems.

### Oil Mapping Algorithm Principles

Previously published research utilizing multispectral imagery for oil thickness determination generally used one of two approaches: multispectral classification where the resulting classes were calibrated for thickness using some external or *in-situ* data (Chouquet *et al.*, 1993; Rogne *et al.*, 1993; Lennon *et al.*, 2006), or the computation of ratios between specific wavelengths and relating the ratio values to oil thickness through laboratory testing (Alhaini *et al.*, 1993; Byfield, 1998). Unfortunately, simultaneous field measurements are usually difficult to obtain during a real oil spill. Additionally, the researchers tended to ignore variability due to background water color and illumination (most studies do not even mention whether the aerial and field data were gathered under sunny or cloudy conditions), and their results tend to be very specific for each particular experiment.

This makes the previous studies of little use in applying them to the development of a real-world, operational system.

OI's initial algorithm development was guided by results of experiments in which nadir-viewing reflectance spectra of known thickness films from several crude oils and Intermediate Fuel Oils (IFOs) were obtained while floating on sea water that was sufficiently deep to eliminate bottom reflectance. The initial data were collected only under sunny conditions with sun angles between 25° and 60°. Representative spectra for Alaska North Slope Crude are shown in Figure 1. The reflectances are the result of three primary contributions: reflectance from the oil film itself, upwelling irradiance of the underlying water column, and the oil's fluorescence. Several general observations relevant to the derivation of crude oil thicknesses from multispectral imagery should be noted from these data:

1. No unique reflectance/absorbance peak was found in the visible-near-IR range which independently changes with varying oil thickness. Additionally, the thinner film oil spectra are significantly attenuated by the underlying water reflectance characteristics.
2. For un-weathered oils, the near-IR range contains very little thickness-related information since the reflectances of both, oil films and background water are very low in that part of the spectrum.
3. The greatest thickness-related change in the oil spectra occur within the 570 nm (green) to 675 nm (red) part of the visible spectrum. Some useful thickness-dependant trends also occur in the UV to 470 nm region.
4. For films over deep water (i.e., no bottom reflectance), very little spectral change was measured with films thicker than approximately 0.15 to 0.2 mm for crudes and IFOs, indicating this is the upper thickness detection limit of an algorithm solely based on UV-Vis-Near-IR wavelengths.

It must be noted that the above observations encompass only the wavelength range of approximately 400 nm to 950 nm, which is the typical span of imaging systems using silicon-based Charge-coupled Devices (CCDs) for image capture. This technology does not allow observations in the deep near-infrared. Some specialized instruments such as NASA's Airborne Visible/Infrared Imaging Spectrometer (AVIRIS) have imaging capabilities at longer wavelengths, and Clark *et al.* (2010) developed methodologies using multiple channels in the 1.2  $\mu\text{m}$  to 2.3  $\mu\text{m}$  range in an attempt to quantify the oil/water ratio and thickness of oil emulsions in AVIRIS imagery collected during the DWH spill.

Following the initial algorithm development, OI conducted further experiments over natural oil seeps in the Santa Barbara Channel, California and at Ohmsett - The National Oil Spill Response Research and Renewable Energy Test Facility, located in Leonardo, New Jersey. OI utilized the Digital Multispectral Camera (DMSC-MkII) imager manufactured by SpecTerra Ltd. in Australia. This frame-grabber type imager uses four lenses and four  $1,024 \times 1,024$  pixels silicon-based CCDs to yield four data channels with 12-bit radiometric resolution. Each channel's wavelength range is customized with 10 nm-wide interference filters (see Table 1 for further specifications).

In the Ohmsett experiments, the imager was mounted approximately 10 m above the tank's water surface from a "crow's nest" tower on a movable bridge across the tank. Increasingly greater quantities of oil were poured onto the water surface within a set of floating containment squares and dispersed to cover each square (surface breeze prevented the oil film thickness to remain completely homogeneous in each square). Because the tank's depth is approximately 2.5 m and its bottom is painted white, the water column's back-reflectance does not represent conditions normally encountered at sea. To better approximate

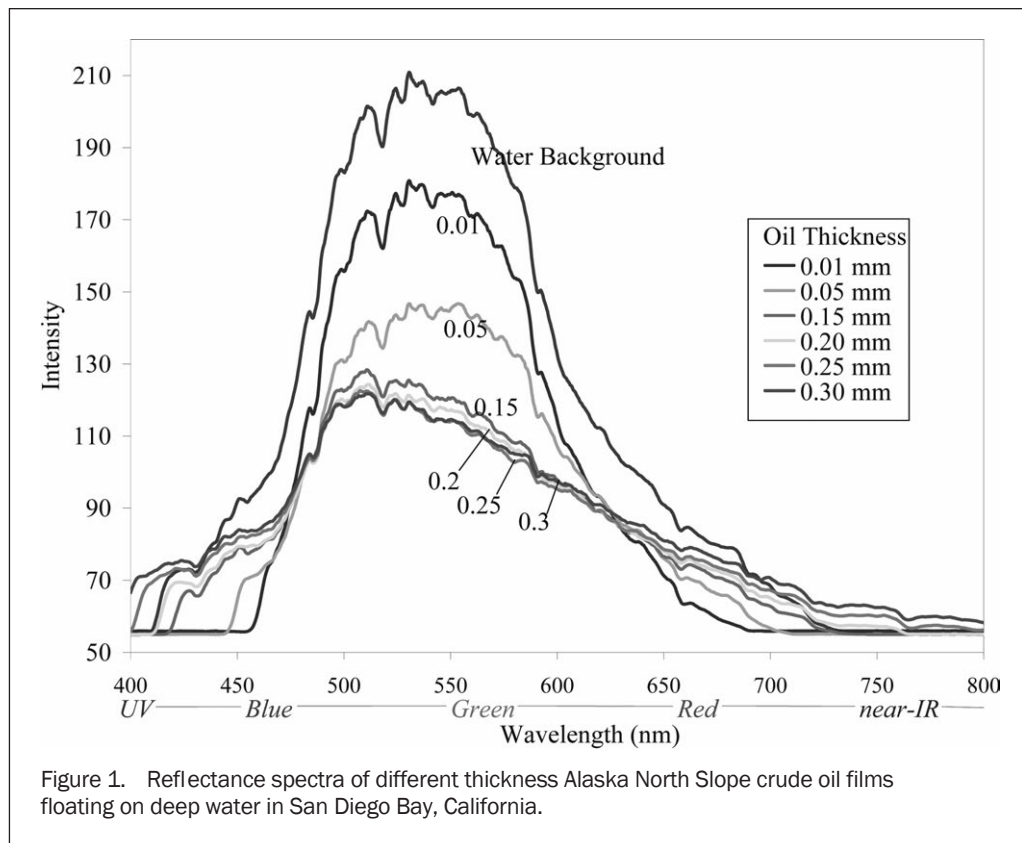


Figure 1. Reflectance spectra of different thickness Alaska North Slope crude oil films floating on deep water in San Diego Bay, California.

TABLE 1. SPECIFICATIONS FOR OI'S SPEC TERRA DMSC M ULTRASPECTRAL IMAGER AND JENOPTIK THERMAL CAMERA

	DMSC Mk-II	Jenoptik IR-TCM640
<b>Detector Type</b>	Progressive-scan CCD	Uncooled Microbolometer
<b>Number of Channels</b>	4 customizable w/10 nm interference filters	1
<b>Image Format</b>	1024 × 1024 pixels	640 × 480 pixels
<b>Spectral Range</b>	400 – 950 nm	7.5 – 14 μm
<b>Dynamic Range</b>	12-bit	16-bit
<b>Thermal Resolution</b>		<70mK
<b>Field of View</b>	29.3° × 29.3°	30° × 23°
<b>Dimensions</b>	25.4 cm × 25.4 cm × 27 cm	153 cm × 91 cm × 111 cm
<b>Weight</b>	16.3kg	1.05kg

background deep-water color and reflectance, a dull canvas tarp painted blue-green was used to cover the bottom of the tank below and around the containment squares. The squares were then imaged as the bridge moved over them (Svejkovsky and Muskat, 2009).

Work over the Santa Barbara Channel oil seeps involved mounting the imaging equipment in aircraft and coordinating simultaneous imaging of suitable oil targets with sampling of the oil's thickness at specific locations from a small vessel. The oil film thicknesses were field-measured using a tank-validated procedure with a clean Plexiglas plate that was dipped through the oil film, retrieved, the adhered oil volume determined, and thickness computed based on the volume and total plate surface area to which the oil adhered (Svejkovsky and Muskat, 2006).

Through experimentation, OI chose 450, 551, 600, and 710 nm to represent a highly efficient channel combination for maximizing the spectral reflectance changes with increasing oil film thickness. The developed oil mapping algorithm is described in more detail in Svejkovsky *et al.* (2008) and Svejkovsky and Muskat (2009). It consists of two steps: The

first step utilizes a neural network classification algorithm applied to the four available DMSC channels to identify all imaged ocean surface areas that likely contain some oil, and to eliminate artifacts caused by sun glint (the most common), high suspended sediment, floating kelp, and seaweeds, etc. The second algorithm, specifically targeting thickness distributions, is then applied only to the pixels believed to contain oil. For each oil-contaminated pixel, it utilizes the deviation of the different available band ratios from the "clear water ratios" (computed in neighboring areas with no oil contamination). The objective is to utilize the ratio deviations from site and time-specific background reflectance (rather than absolute ratio values as was done in previously published studies) to better account for regional differences in water color and illumination characteristics. The thickness-determining algorithm utilizes a fuzzy ratio-based classification to assign each pixel into a thickness range based on the multiple ratios. The actual thickness classes are assigned based on data from experimentally or field-derived look-up tables stored in the algorithm. Most commonly four to six thickness classes can be derived up to the 0.15+ mm upper

thickness determination limits. The algorithm was validated in the field off Santa Barbara and at Ohmsett (Svejkovsky and Muskat, 2009).

OI conducted additional research to add a thermal IR camera to the multispectral system in an effort to both increase thickness determination efficiency and to extend the upper thickness measurement range to more than approximately 0.15 mm. OI used a Jenoptik IR-TCM-640 camera which provides internally calibrated 640 pixel  $\times$  480 pixel images with 16-bit dynamic range and 0.07°C thermal resolution at 7.5  $\mu\text{m}$  to 14  $\mu\text{m}$  (see Table 1 for further specifications). Ohmsett experiments were conducted during the summer under both clear and cloudy skies and various sun angles (with surface water and air temperatures ranging 26°C to 27°C and 21°C to 28°C, respectively), and winter under similarly varying sky conditions (with water and air temperatures ranging 2.4°C to 4.5°C and 3.5°C to 5.5°C, respectively). The tests determined that the approximate daytime lower oil detection limit for IR imaging is in the range of 0.01 to 0.02 mm (i.e., thinner oil films are indistinguishable from the surrounding water temperature). This determination agreed with previously published estimates (Hurford, 1989; Belore, 1982). It also implied that significant overlaps exist between the minimal crude oil thickness detection possible with IR imagers and the maximum thickness determination limit of visible wavelength range systems. In OI's experiments, the aforementioned flip in the oil's thermal signature from cooler to warmer than surrounding water occurred within the overlap range (in agreement with previously published reviews such as Fingas and Brown (1997), and the relationship between increasing thickness and increasing apparent temperature appears linear (the maximum routinely tested thickness of fresh oil at Ohmsett was 2 mm). This allows utilization of the multispectral visible wavelength overlap data to "calibrate" the IR band for thickness. As was already noted, changes in reflectance properties within the visible to near-IR spectrum allow thickness-related differentiations to be made with the multispectral sensor up to around the 0.15 mm range, after which the color of the oil films no longer changes appreciably. In the thermal imagery sheens and very thin films are not readily differentiated, but thicker films exhibit distinguishable thickness-related thermal emittance trends, well past the differentiation limits of the visible-near-IR multispectral imager. Figure 2 shows algorithm validation results from Ohmsett experiments in which known volumes of Alaska North Slope crude oil were poured into the containment squares, the oil was spread out in each square and allowed to form patterns of different thicknesses. The squares were then imaged, classified for oil thickness and the total oil volume in each square was calculated from the classification. The results underscore the utility of combining the multispectral visible-near-IR imagery with thermal-IR imagery to achieve better overall accuracy as well as extend the thickness measurement range.

OI's (daytime) thermal IR imaging tests showed a consistent increase in apparent temperatures in increasingly thicker oil films up to the tested 2 mm. The relationship was observed during summer and winter conditions and under both clear and cloudy skies (the slope of the thermal oil-water contrast versus thickness varied with solar input conditions but could be compensated by an offset determined from the visible to near infrared channel overlap range). This is in contrast to Brown *et al.* (1998) who reported no correlation between oil film thickness and thermal signal strength. They based their conclusion on comparisons of thickness measurements within tank-contained slicks made with a subsurface acoustic probe, and relative contrast differences between oil and surrounding

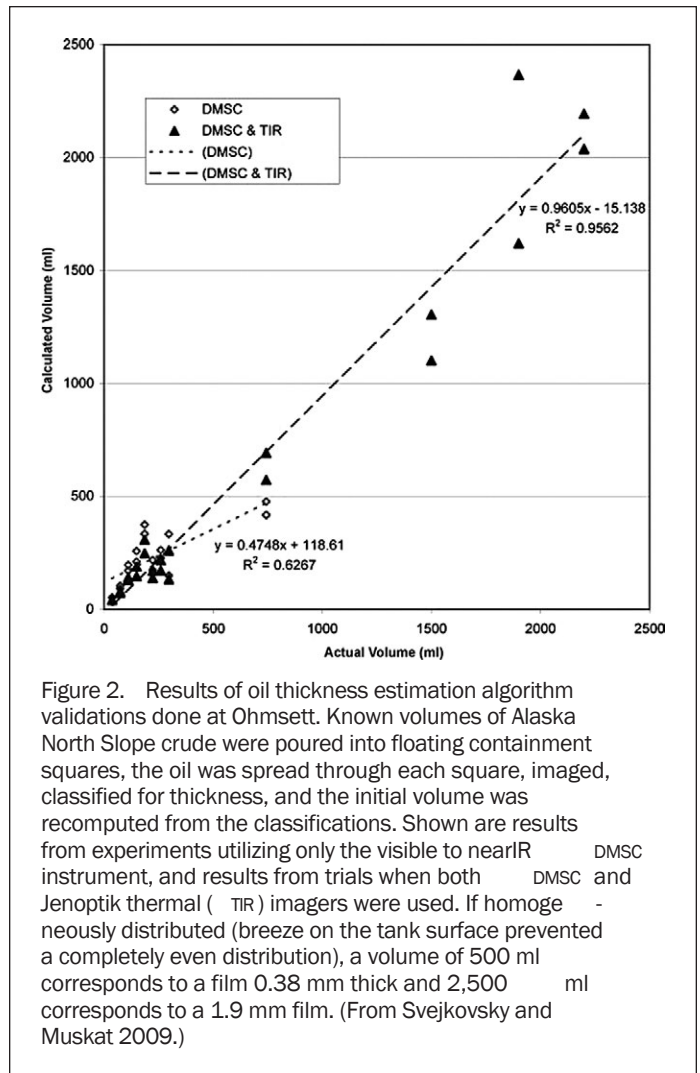


Figure 2. Results of oil thickness estimation algorithm validations done at Ohmsett. Known volumes of Alaska North Slope crude were poured into floating containment squares, the oil was spread through each square, imaged, classified for thickness, and the initial volume was recomputed from the classifications. Shown are results from experiments utilizing only the visible to nearIR DMSC instrument, and results from trials when both DMSC and Jenoptik thermal (TIR) imagers were used. If homogeneously distributed (breeze on the tank surface prevented a completely even distribution), a volume of 500 ml corresponds to a film 0.38 mm thick and 2,500 ml corresponds to a 1.9 mm film. (From Svejkovsky and Muskat 2009.)

water recorded with an un-calibrated, 8-bit downward-looking analogue thermal camera/VHS tape system. Since the camera yielded only relative brightness and had automatic gain control, it is not known what thermal range each video frame represented (which also contained various solid objects in addition to the water and oil), and hence the thermal increment represented by each greyscale. It is possible that any thermal trend was masked within the 25 to 38 greyscale range of the data (10 to 15 percent range of highest grey level) by frame-to-frame variability in the thermal resolution of the 8-bit images. Perhaps more importantly, however, the vast majority of the measurements were over oil slick portions thicker than 2 mm (and up to 8 mm), i.e., outside the range of our own Ohmsett tests. It is possible that under given solar input conditions the increase in heat emission becomes asymptotic for films exceeding several millimeters. We intend to conduct further research on this subject.

The developed multi-sensor system and processing algorithms were first utilized operationally in California during a crude oil spill from Platform "A" in the Santa Barbara Channel in December, 2008, and an IFO spill during ship-to-ship bunkering operations in San Francisco Bay in October 2009. The total volume of oil spilled in the two incidents is still under investigation, however, all estimates indicate that the Santa Barbara Channel spill (the larger of the two) totaled at most a few thousand liters of crude,

affected a few square kilometers of ocean surface, and direct recovery and associated response operations could terminate after a few days.

## Methodology Adaptations for the Deepwater Horizon

### Spill Response

Under direction from the National Oceanographic and Atmospheric Administration (NOAA) and British Petroleum (BP), OI was mobilized to aid the DWH Spill response on 01 May 2010. Following equipment installation on-board a NOAA Twin Otter aircraft, the oil mapping system was first utilized on 04 May 2010. In the following days, until 26 July 2010, the OI imaging and NOAA aircraft teams flew one to two imaging missions almost daily, based out of Mobile, Alabama. The imaging equipment consisted of the DMSC MKII multispectral sensor configured with a 450, 551, 600, and 710 nm filter combination, and a Jenoptik IR-TCM640 thermal IR camera system. Both imagers were integrated with an Oxford Technologies 2502 DGPS/IMU positioner with 100 MHz update rate and 2 m circular positioning error under Space Based Augmentation System (SBAS) conditions. OI's custom software was used to auto-georeference and mosaic the acquired image frames. Previous tests with this system configuration and software showed RMS positioning error after the auto-mosaicking of <6 m at 3,040 m flight altitude (Svejkovsky and Muskat, 2009). Most offshore oil mapping missions were conducted at 3,800 m altitude, resulting in 2 m data resolution for the DMSC and 4 m resolution for the Jenoptik IR imagery. Beached and shore-entrained oil mapping missions were conducted at approximately 1,700 m, yielding approximately 0.7 m and 1.5 m spatial data resolutions, respectively.

As was already mentioned, the oil mapping system was previously used operationally on two spills in California. In both cases, the imaging required merely one to five flight lines of a few kilometers in length to completely image the spill-affected area. At 2 m resolution, the DMSC imaging swath is 2,048 m and some overlap is required between adjacent image lines for proper multi-line mosaicking. Already on 04 May 2010 the size of the DWH spill precluded any attempts to map the complete spill area. Since sunglint severely degraded image usefulness of visible wavelength imagery from the DMSC sensor, imaging was limited to several hours in the morning after sunrise and several hours in the afternoon before sunset when low sun angles prevailed. (The thermal IR imagery is not affected by sunglint and could be used throughout the day and night.) These spatial and temporal limitations dictated that the OI team received guidance on which specific target areas within the spill area to image each day. Initially, such guidance and target area prioritization was received independently from the multiple Incident Command Posts (ICPs) that were established. Later in the spill, the Houma, Louisiana ICP became the lead center for guiding the various remote sensing missions.

Another methodological problem that was immediately recognized during the spill was the need for very fast and broad distribution of the image-derived analyses. The prime reasons for this were (a) the immediate need for any oil thickness and location information to help guide on-water recovery operations, trajectory models, etc., and (b) to provide access to the data and analyses for the geographically very dispersed response community. The immediate analysis generation need was hampered by data processing difficulties due to the extreme haze, sun angle and (on some flights) overhead cloud-caused illumination imbalances which affected the visible wavelength image quality. Flight

takeoff timing (often at first light), length, and other logistics also prevented the collection of adequate pre-flight and in-flight calibration data that are normally used for standard application of the above-described oil thickness classification algorithm. These factors contributed to the need for additional, manual processing procedures to maintain quality control and flight-to-flight oil map product consistency. On the other hand, OI's discussions with the various end-user groups made it clear that most of the image-derived product end-users did not have an immediate need for products with highly detailed oil thickness classifications. Instead, the specific need was to quickly obtain GIS-compatible maps of recoverable oil (i.e., relatively thick or emulsified) versus unrecoverable (i.e., sheen). For this reason, the OI team developed a "Rapid Turn-around" class of analysis products that highlighted all imaged oil features thicker than approximately 0.1 mm as a single class. These analyses could be consistently derived much faster from the imagery data and were usually generated in-flight while flying back to the aircraft base in Mobile, Alabama. They were then disseminated as e-mail attachments to a recipient list immediately upon landing.

Following each flight, the acquired data were then reprocessed for multiple oil thickness classes, although the unavailability of calibration data and the sometimes extreme humidity/haze conditions resulted in most data sets to be confidently classified into only four or less thickness range classes. These "Rapid Turn-around" and fully classified products were then made directly available to the situation desk and operations unit at the Houma ICP and to the broader response community through the Environmental Response Management Application<sup>®</sup> (ERMA<sup>®</sup>) web mapping application established by NOAA early in the response. Sample Rapid Turn-around and Full Classification products of the oil spill source area are shown in Plate 1.

ERMA<sup>®</sup> is a web-based mapping application that was designated as the US Government's Common Operating Picture (COP) providing real-time situational awareness to the Government and partner agencies across the response. Data from multiple sources were loaded daily or multiple times a day into a common framework. ERMA<sup>®</sup> provided response and baseline data in this common web-based visualization tool. OI and other remote sensing data products were made available for USCG Command briefings at the Unified Area Command (UAC) and at the ICPs as well as to the National Incident Command (NIC) in Washington, D.C. The incorporation of these data resources supported real-time decision making at all levels of the response as well as for the injury assessment and the subsequent restoration planning that are currently ongoing. ERMA<sup>®</sup> was jointly developed by NOAA and the University of New Hampshire.

### Results and Lessons Learned

The OI system was found to be effective in mapping areas of fresh and slightly weathered oil, oil emulsions, and beached or land-entrained oil in various stages of weathering. Plate 2 shows an area containing recently upwelled, unemulsified oil near the Spill Source site, as imaged by OI's multispectral visible-near-IR and thermal IR systems on 06 May 2010. The region generally contained areas of thick, fresh oil which appeared dark brown to the human eye and yellow when rendered with the DMSC's 450, 551, 600 nm for the blue, green, and red components, respectively. In concurrence with OI's previous experimental observations, sheens tended to exhibit elevated reflectances (from surrounding water) in the 450 and 551 nm bands, while thick oil films exhibited suppressed reflectance in the 450 nm, and elevated reflectances in the longer wavelength bands, particularly the

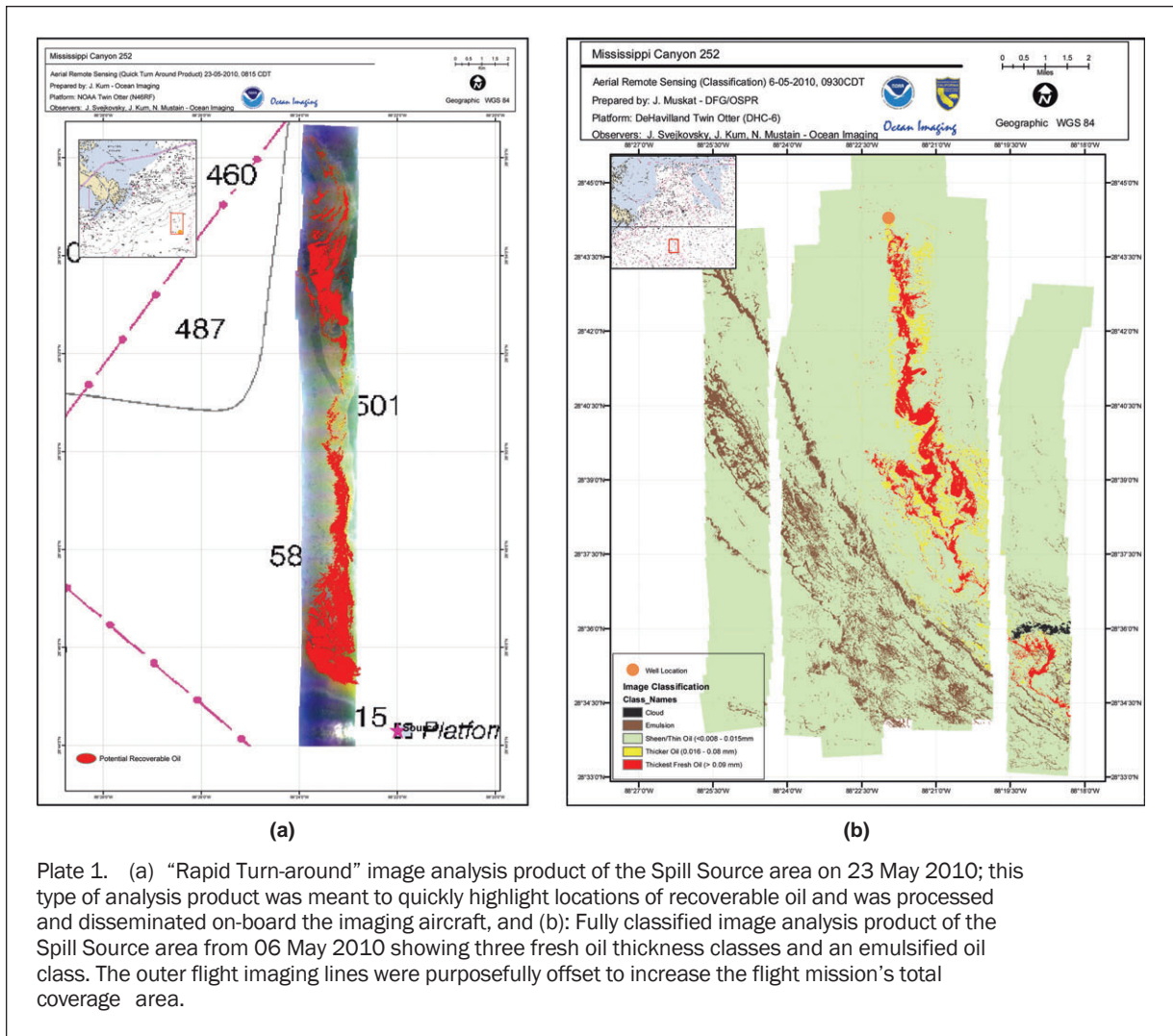


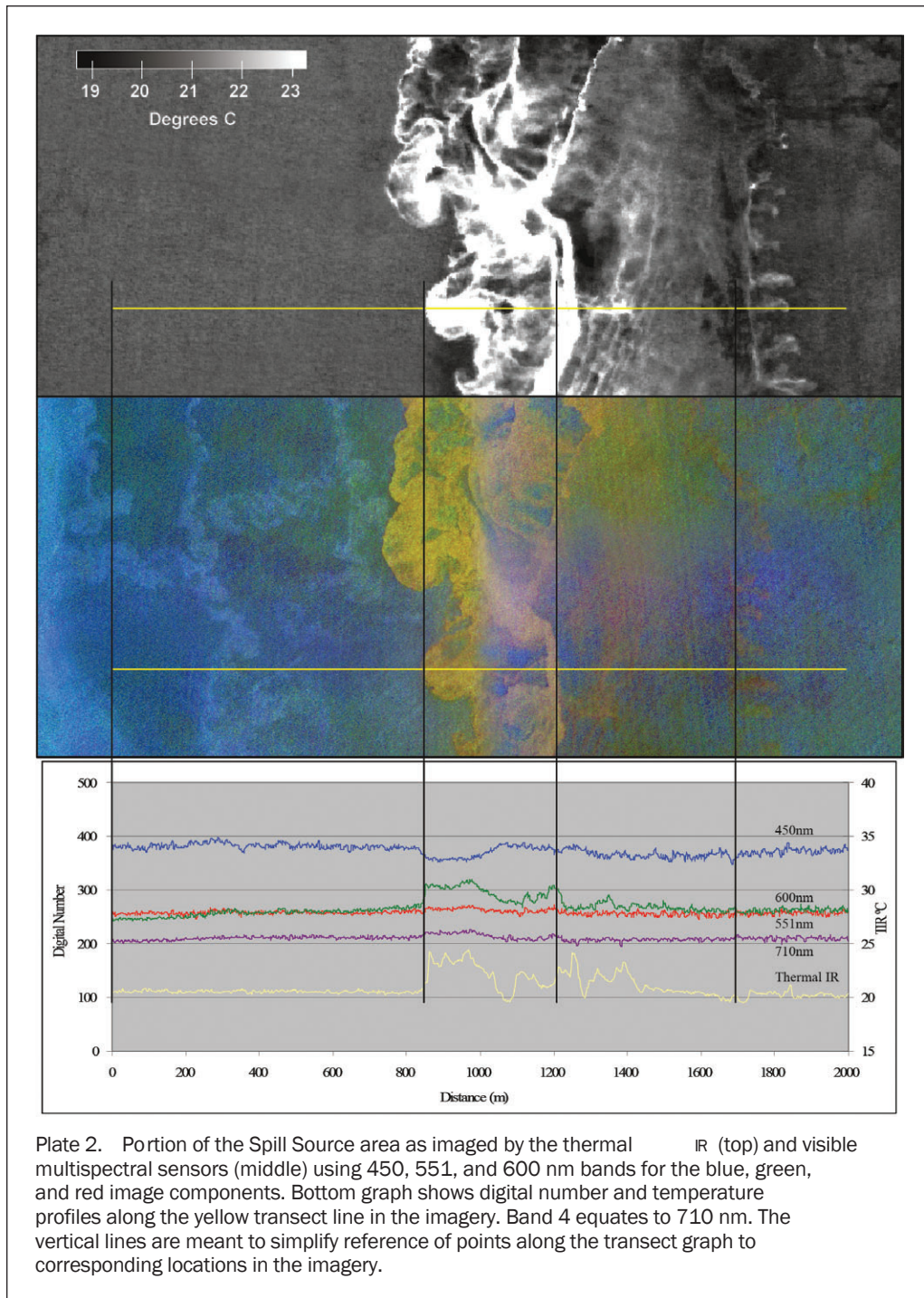
Plate 1. (a) “Rapid Turn-around” image analysis product of the Spill Source area on 23 May 2010; this type of analysis product was meant to quickly highlight locations of recoverable oil and was processed and disseminated on-board the imaging aircraft, and (b): Fully classified image analysis product of the Spill Source area from 06 May 2010 showing three fresh oil thickness classes and an emulsified oil class. The outer flight imaging lines were purposefully offset to increase the flight mission’s total coverage area.

551 nm channel. Early in the response, the thick oil exhibited an IR signature up to several degrees Celsius warmer than the surrounding water. Thinner oil, approximately 0.01 to 0.04 mm thick, as estimated by OI’s Ohmsett experiments and others’ previously published work, appeared cooler by at most a few tenths of a degree Celsius. Very thin oil films, less than approximately 0.01 mm based on previous experimental results, could not be distinguished from the water background in the multispectral visible bands. Very thin sheens were difficult to distinguish from clear water even in the multispectral data, partly due to heavy atmospheric haze that negatively affected the multispectral bands, but also because in many cases, they likely covered essentially the entire ocean surface not covered by thicker oil; hence there were no true “clear water” pixels from which to differentiate the signal levels.

As OI also found to be the case in the previously imaged spills in California waters, the thermal imagery can be relatively easily utilized for rapidly mapping oil features thick enough to be recoverable with the available boom and skimmer resources. The thermal oil signature of freshly upwelled oil near the Spill Source was, however, found to be affected by sea state, since rough seas apparently caused the thick oil to both disperse faster into

thinner films and also to become periodically submerged and lose its heat content. Another factor that we believe caused variability in the thermal signature of the freshly upwelled oil is the application of subsurface dispersants at the point of release on the seafloor. The data shown in Plate 2 were obtained before sustained subsurface dispersant injections began, and thus show thermal and multi-spectral signatures void of any dispersant effects. Later in the spill, the thick fresh oil areas near the Source Site tended to have a less distinct and more uneven heat signature in the thermal data, and often appeared to be more submerged to the naked eye. We postulate this could be due to the effects of the injected dispersants on the oil mixture that did make it to the surface.

OI’s oil thickness classification algorithm was developed for fresh or only mildly weathered oil films. No attempts were thus made to estimate the thickness of oil emulsions, other than to identify them as such in a single “emulsion” class. For the purposes of the image-based oil maps, emulsions were defined as being highly reflective in the near-IR 710 nm band (versus thick fresh crude oil which has only slightly elevated reflectance (Figure 1 and Plate 2)). To the naked eye, emulsions appeared most commonly as bright, orange-red-hued features. Sometimes areas of very dark, likely heavily weathered tar-like oil also appeared within



the bright emulsion features. Plate 3 shows representative multispectral and thermal IR data of an offshore area containing emulsions. The presence of emulsions in this and other areas imaged at other times was qualitatively field-verified by communications from response vessel crews operating in the area. Using the DMSC's 450, 551, and 600 nm channels for blue, green and red components, respectively, the thickest emulsions appear dark purple and the thinner accumulations appear bright red. Relative to clear water areas (likely covered by very thin oil sheen), the emulsion features show depressed reflectances in the 450 and 551 nm bands and increased reflectance in the 600 and 710 nm bands. As was already noted, Clark *et al.* (2010)

subsequently developed an emulsion composition and thickness estimation algorithm based on reflectance spectra of laboratory re-mixed emulsions from an initial DWH sample collected in the field. The algorithm relies on deep near-IR wavelengths available on the hyperspectral AVIRIS instrument but not available with imagers utilized by OI during the response.

Previously published literature tends to state that oil emulsions generally cannot be discerned in thermal IR imagery due to their high water content, which tends to eliminate any thermal contrast between the oil film and the surrounding water. The review article of Fingas and Brown (1997) is often cited as a reference, in which the statement is

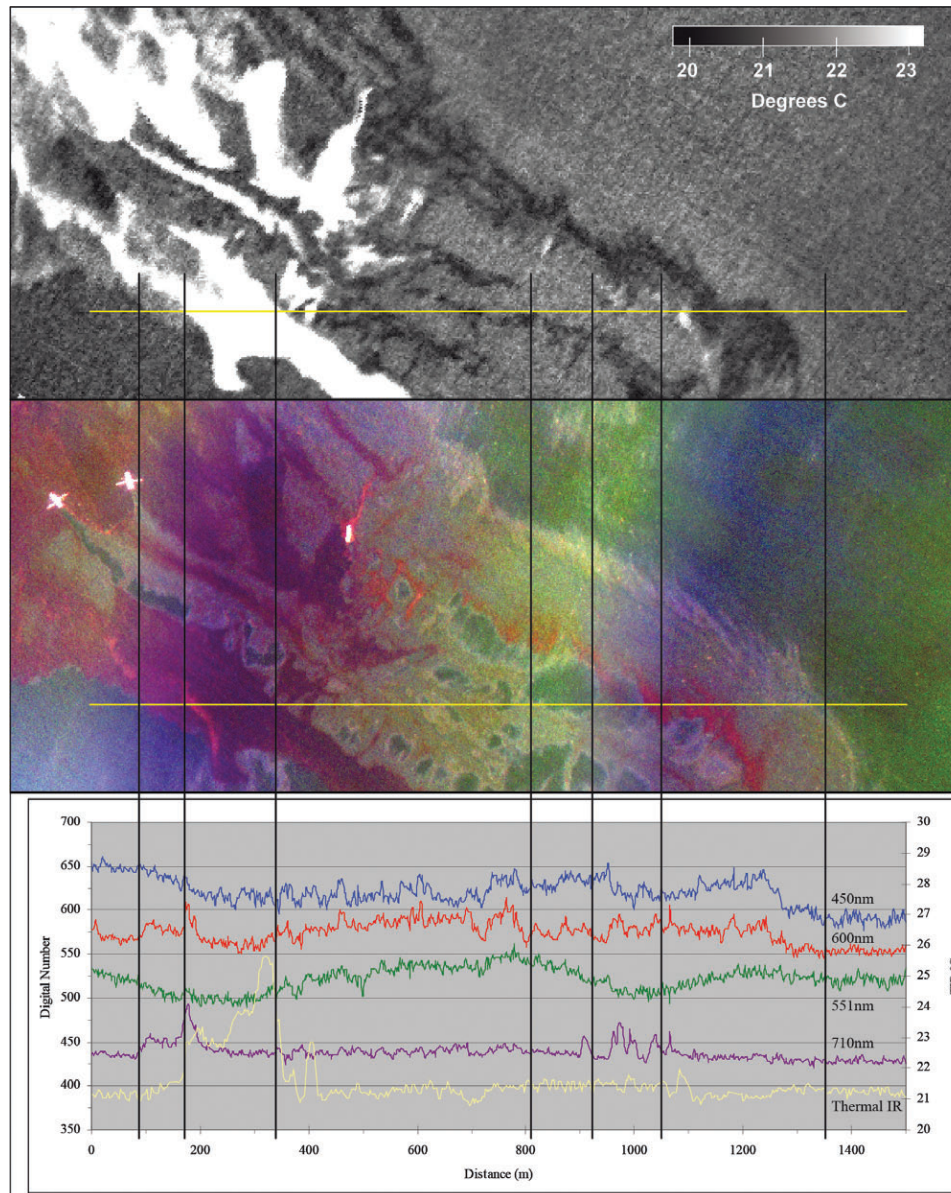


Plate 3. Region containing emulsified oil of different thicknesses and textures, as imaged by the thermal IR (top) and visible multispectral sensors (middle) using 450, 551, and 600 nm bands for the blue, green and red image components. Bottom graph shows digital number and temperature profiles along the yellow line in the imagery. Band 4 equates to 710 nm. The image contains a pair of vessels towing a boom corralling the emulsions for recovery. The vertical lines are meant to simplify reference of points along the transect graph to corresponding locations in the imagery.

linked to work by Bolus (1996). Both, OI's experimental data from Ohmsett with artificially created oil emulsions, and thermal imagery obtained during the DWH spill do not support this contention. At Ohmsett, under partly cloudy and fully overcast conditions and 20°C/16.5 to 19.5°C air/water temperatures, emulsion films containing 20 percent water exhibited thermal signatures similar to pure oil films. Emulsions containing 60 percent water showed a positive thermal contrast compared to water at approximately 0.3 mm and greater thicknesses. In image data containing DWH emulsion features, demonstrated in Plate 3, thin oil emulsions appear slightly cooler than water, similar to thin fresh oil films

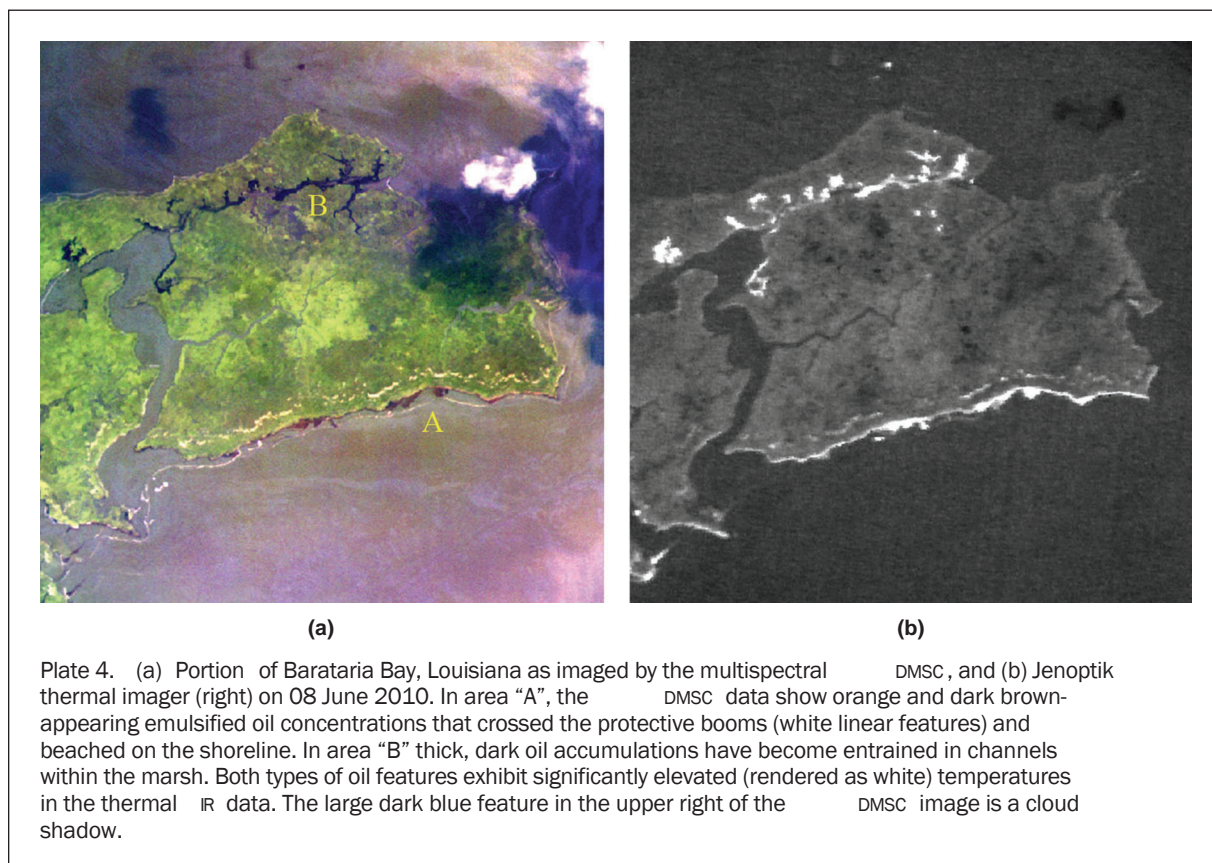
despite their being vastly different in color reflectance. Thick emulsion accumulations appear to trap heat during the day and thus appear much warmer than the surrounding ocean surface. More quantitative analysis of the OI aerial system's imagery with respect to DWH emulsion field samples and ancillary measurements collected during the DWH response by SL Ross Environmental Research Ltd. (Belore *et al.*, 2011) are presently on-going. They also support the premise that floating oil emulsions within a relatively wide range of thicknesses and oil/water ratios can be detected (and some quantitative information extracted) by a modern thermal imager in the 7.5  $\mu\text{m}$  to 14  $\mu\text{m}$  spectral range.

OI's aerial system was also tasked on multiple occasions to scout various shoreline regions for beached oil, and map oil accumulations which have become entrained within the marsh channels of the Mississippi Delta. The oil distribution classifications were then relayed to each region's Shoreline Cleanup Assessment Technology (SCAT) teams either directly or through the ERMA<sup>®</sup> site and were then utilized to help guide the next-day's field operations. Some of the heaviest shoreline and inter-marsh oiling occurred in and around Barateria Bay, Louisiana. Plate 4 shows representative multispectral visible and thermal data from that region. The mapping of oil features along the shoreline and within the marshes required higher spatial resolution imagery than the offshore oil mapping, because the beached accumulations were often elongated along the beach and thus much narrower than the commonly wider, more spread-out offshore oil targets. OI hence conducted its imaging at lower flight altitudes, corresponding to spatial resolutions of 0.7 m and 1.5 m for the DMSC and Jenoptik cameras, respectively. Obviously, such resolutions still compromised the detection of the smaller oil accumulations, but were deemed a reasonable compromise between the need for high spatial resolution and useful daily spatial coverage acquired within the acceptable flight time and sun angle limits.

As can be seen from the data shown in Plate 4, beached or entrained accumulations of orange-colored emulsions and thick, dark weathered oil could be readily detected in the multispectral data as well as in the thermal imagery where such accumulations usually appeared warmer than the surrounding land and water by several degrees Celsius. Unlike in the offshore areas, however, the added complexities of vegetation and land features with highly variable visible/near-IR light reflectance and thermal IR emission

characteristics produced many more potential false targets. For example, heavy beached accumulations of dark organic matter such as dead eel grass had visible and near-IR reflectance characteristics very similar to the dark, thick oil accumulations in both the DMSC data and the naked eye. The thermal IR often provided differentiation capabilities, since the weed accumulations tended to have much lower heat emission characteristics than was typical for dark, weathered oil. Such considerations precluded the application of any automatic oil-detection algorithm without significant manual editing by the OI image analysts. In a number of instances after the earliest shoreline/marsh mapping missions, OI worked interactively with some of the SCAT teams by providing them with coordinates of uncertain oil-like targets and having the SCAT personnel report back on the true identity of the targets after their field work the following day. This greatly aided in "fine tuning" the image classification procedure to better eliminate potential false targets specific to the Mississippi Delta environment in future data sets. It should be noted that the available combination of visible, near-IR and thermal IR wavelengths proved much more effective in accurately mapping oil in the marsh areas than would have been possible with only the visible/near-IR or thermal IR imagery alone.

The unprecedented and novel daily availability of the aerial multispectral imagery and oil thickness/weathering state classification products initially met with skepticism in some cases, but also faced the formidable obstacle of initially not having established protocols for their utilization within the various response groups and activities. However, the response groups in multiple command centers and in the field soon began to formulate strategies to take advantage of the new type of information. As awareness of the OI analyses grew, so too did the demand for including multiple



target areas in each day's mission. The following applications exemplify diverse successful utilizations of the OI aerial system:

### **Determination of Regional Oil Volume and Trajectory**

The aerial imagery acquired over the Spill Source site was commonly utilized to establish the daily pattern and relative quantity of oil emanating to the surface. With limited imaging time, the multiple flight line image acquisitions were adjusted on-site to match the direction of the heaviest oil distribution and document the pattern and trajectory direction of the main oil slick. One such analysis is shown in Plate 1b. (As the Plate 1b sample demonstrates, the imaging swaths were sometimes purposely offset to increase the overall spatial coverage of the Spill Source imaging missions.) The multispectral/IR imagery and thickness classification products were further augmented by OI's capture of carefully framed oblique images (using digital SLR cameras) and written observer reports (which helped to extend the "information horizon" beyond the immediate limits of the image and classification data sets). These three combined elements were especially helpful to the Houston ICP where they heightened situational awareness and contributed significantly to the safe conduct of simultaneous operations (SIMOPS) in the source area. In particular, the multispectral imagery and thickness classes were integrated with surface SIMOPS charts by the survey support team in Houston and these, together with the obliques and observer reports, were transmitted to the offshore captains to aid them in visualization of the relative positions of the many surface vessels and the upwelling oil.

The data were also utilized by NOAA's oil distribution modeling team to supplement information from visual observations produced by the NOAA trained observers flying from several forward locations along the coast.

Satellite SAR and airborne SLAR imagery were used extensively to track the spatial extents of the DWH spill. In mid-May the imagery began to show an extension of the overall slick expanding southward into the Gulf of Mexico, raising fears that the oil will be entrained in the Gulf of Mexico Loop Current and thus be transported eastward to ecologically sensitive areas such as the Florida Keys. Because SAR imagery does not provide information on the state or thickness of the oil causing the low-backscatter signature, the SAR data could not by itself be used to evaluate the magnitude of the inherent threat. NOAA (and other response groups) thus directed the OI system to document the state of oiling along the southern periphery of the SAR-derived oil slick boundary.

The magnitude of the oil spill extent prevented the OI team from contiguously mapping the entire area. Instead, with visual observation showing that the vast majority of the southernmost SAR-sensed oil slick feature is due only to very light sheen, imaging was done only over features representing thicker oil. All the features corresponded to relatively light emulsion accumulations. The detailed aerial maps allowed the evaluation of the relative amount of oil nearing the Loop Current boundary. The combination of large-scale SAR or SLAR-derived imagery and aerial multispectral/IR imaging was utilized several more times during the DWH spill response, each time with multispectral imagery being used to determine the state or type of oiling within a feature of interest initially revealed by the SAR data.

A unique use of the imagery was as a check on the effectiveness of subsurface dispersant application. Because the Twin Otter/OI platform maintained a consistent observational record of the surface oil above the source, it provided a history of relative surface volume. Typically, untreated oil

would reach the surface from the leaking riser in a matter of a few hours, while the reduced droplet size of effectively treated oil would slow the rise time indefinitely. By examining the surface slick before and a few hours after commencement of subsurface dispersant use, a qualitative assessment of effectiveness can be made. The imagery and image-derived oil thickness analyses were utilized as part of Environmental Protection Agency-sanctioned evaluation of the subsurface dispersant application concept early in the response.

As was noted above, the Rapid Turn-around analysis products identifying potentially recoverable oil features were produced in-flight by the OI team and disseminated as e-mail attachments immediately upon landing, as well as being loaded into the ERMA<sup>®</sup> COP within hours. By June 2010 the list of recipients also included a number of at-sea vessels taking part in the offshore recovery operations who thus gained rapid access to the aerial image-based information.

### **Imaging of Aerial Dispersant Applications**

Aerial dispersants were heavily utilized throughout the spill response. Plate 5 shows data from an imaging flight coordinated with the dispersant application team. To eliminate the risk of direct contact with personnel, aerial dispersant releases were usually conducted a considerable distance from the Spill Source area which contained the highest concentration of vessels and crew. This resulted in most of the dispersant being released on weathered and emulsified oil. Although there has been debate in the past whether aerial dispersant applications can be effective on oil emulsions, OI's imagery supported the notion that, at least in the DWH spill, Corexit 9500 aerial dispersant application on floating oil emulsions was likely effective under wind and sea-state conditions existing in the imaged region. Plate 5 shows image data from a single flight line that transected a region containing concentrations of emulsified oil (appearing bright orange to the naked eye), and a neighboring region that had been sprayed with dispersant approximately 30 minutes before the image acquisition. Visual observations showed both a color and textural change upon application of the dispersant: the oil substance changed from a bright orange to yellow in appearance, and began to be drawn out into thin striations by the near-surface wind-induced current. The color changes were also recorded in the multispectral imagery, but the most dramatic change was documented by the thermal IR imager. The un-dispersed floating emulsions had a typical, distinct cooler-than-water signature (indicating relatively thin films). This signature was completely lost in areas affected by the dispersant spray, suggesting that the dispersant-affected oil had submerged into the water column which the thermal imager cannot penetrate. The imagery acquired in conjunction with both, aerial and subsurface dispersant applications continues to be used by multiple groups evaluating the effectiveness of dispersants in the DWH incident and the utility of dispersants for future spills.

### **Mapping of Beached and Land-entrained Oil**

One of the most useful aspects of the marsh imaging missions to the field response crews was the imagery's ability to reveal oil accumulations deep within the marsh channels. In many cases such channels were quite difficult and very time consuming to scout by field crews in vessels, and could not readily be reached by foot. The image-derived oil distribution maps could thus be used to direct and thus maximize efficiency of the field SCAT resources.

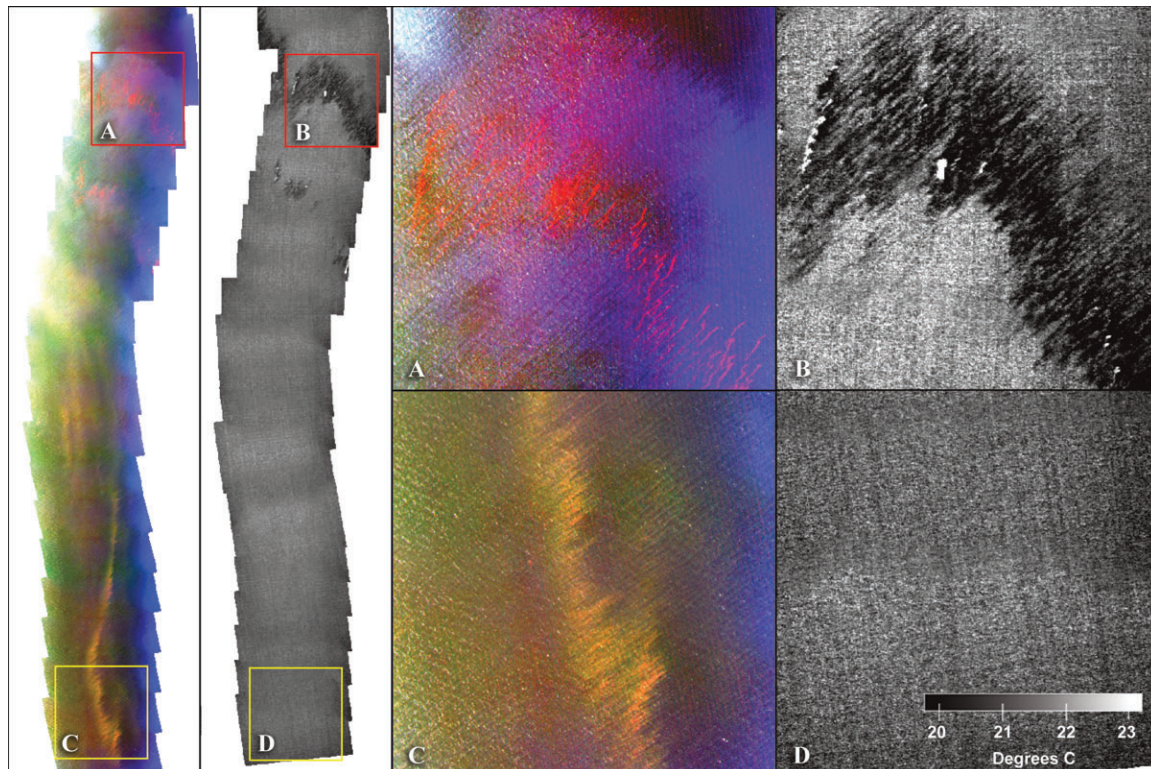


Plate 5. Multispectral color (450, 551, and 600nm) and thermal imagery along a flight line that transected an area with emulsions where no dispersant was applied (top) and a region where dispersant was sprayed over floating oil emulsions approximately 30 minutes before (bottom). At right are enlargements of portions of the flight line showing the un-dispersed oil (A = multispectral, B = thermal), and dispersed oil (C = multispectral, D = thermal). Most of the un-dispersed emulsions exhibit a cooler-than-water thermal signature (thinner), with a few smaller areas appearing warmer (thick). The dispersed oil had likely sunk into the water column and is thus no longer discernible in the thermal data.

Following initial coordinated field validation efforts between the OI imaging team and SCAT teams surveying several island shorelines in Barataria Bay, OI overflights were conducted to guide future SCAT surveys. As mentioned above, OI oil thickness and distribution maps were available to response personnel through the ERMA<sup>®</sup> viewer. Additionally, OI's oil distribution and thickness maps were transmitted directly using email to the SCAT Unit coordinators in KMZ file format for direct viewing in Google Earth<sup>™</sup>.

### Imaging System Limitations

The greatest recognized shortcoming of the OI aerial imaging system was the limited area that it could image each day, which limited, in turn, the number of response groups or activities that could utilize each day's image analysis products. For example, if the OI system was tasked to image sections of the Mississippi Delta marshes to aid that region's SCAT and Natural Resource Damage Assessment (NRDA) teams, the system could often not be utilized that day for aiding offshore oil recovery operations. In an attempt to take full advantage of the capabilities of the OI system and crew, data collection over specifically requested areas and targets of opportunity was also often conducted on the out-bound and in-bound legs of flight missions primarily intended to image the source or some impacted length of shoreline.

MODIS, SAR, and SLAR imaging platforms provided daily broad, synoptic views of the interpreted slick extents, but

were unable to provide thickness classifications or discriminate between sheen and thicker recoverable oil. Conversely, the OI system was providing daily or twice daily (weather permitting) location-focused, data sets and detailed thickness class analyses, but was limited in geographic scope to a total collection footprint of 350 to 500 km<sup>2</sup> per flight mission. As a consequence, an attempt was made to bridge the information gap between the two available remote sensing options using available (off-the-shelf) large-format aerial mapping systems that (although unable to provide a synoptic view of the full slick extents like SLAR, or detailed thickness classes like OI) could provide on-demand, multispectral, intermediate-scale, low-latency imagery data over operationally significant marine and/or shoreline areas of up to ~5000 km<sup>2</sup> per day (daylight and weather permitting). One such system tested was the Leica ADS40 which was optimized and flown by Northrup Grumman to acquire and deliver (within several hours of acquisition) four-band (visible and near-IR) orthoimagery with a ground sample distance of approximately 5 meters (after ~100:1 pixel aggregation).

The test-use of the large-format photogrammetry systems proved to have three prime hindrances for daily, operational use, however: (a) Not being specifically designed for oil spill mapping, there was no postprocessing mechanism to generate oil-specific analysis products from the data. The system operators simply provided raw, unclassified imagery, limiting its use and interpretation to a few specialists; (b) the data files were too large (several hundred MB, even when

compressed at reduced spatial resolution) for practical mass dissemination to the broad response community as e-mail attachments or web-based ERMA<sup>®</sup> downloads; and (c) No thermal IR image component was available which, as is discussed below, proved highly useful for oil thickness characterizations under operational conditions. It should be noted that the test deployments of the large-format photogrammetry systems (as well as non-operational data acquisitions by hyperspectral systems like NASA's AVIRIS) were in most cases initial attempts at their utilization strictly for oil spill mapping, and their utility will likely increase with more research and experience. In the OI system case, oil spills covering 700 to 1,000 km<sup>2</sup> can be likely fully covered in two missions each day. In spills generating slicks beyond this size extent (as in the case of the DWH incident) only portions of the entire region can be effectively imaged, processed and disseminated as oil characterization analyses.

Collaborative feedback between the OI data acquisition/processing crew, and SCAT and Natural Resource Damage Assessment (NRDA) teams also revealed an important limitation of the use of multispectral/thermal imaging for identifying oiled land areas during the DWH spill. The oil mapping procedures utilized by OI relied on the ground substrate's alteration in visible/near-IR reflectance and thermal IR emittance properties directly caused by the presence of oil. In marsh areas subject to tidal flushing the amount of oil adhering to the substrate after one or more tidal cycles was variable, especially in areas covered with marsh grasses that could be fully, partially, or only intermittently coated with oil residue. While heavily coated grass regions were identified in the imagery with apparently good consistency, lightly coated regions were difficult or impossible to separate from surrounding unaffected marsh. One concept suggested but not attempted during the spill response is to try to identify the oil's presence on flora indirectly through changes in plant stress, as measured by changes through time in indices such as the Normalized Difference Vegetation Index (NDVI) (Rouse *et al.*, 1973). With the voluminous field data collected by the various SCAT and NRDA teams and imagery time series suitable for NDVI change analysis collected by OI as well as several other sources, the concept invites further investigation. Another possibility is the addition of a UV-sensing camera to the system that could potentially reveal hydrocarbon fluorescence on the plant leaves and stems.

## Conclusions

Experience gained through the operational application of OI's multispectral oil mapping system during the DWH spill invites a number of main conclusions about the utilization of such aerial remote sensing as part of oil spill response:

- An aerial system combining visible-near-IR multispectral and thermal IR imaging capabilities can provide information useful for a multitude of spill response activities. This assumes, as was the case with the OI system, that instead of providing the response community with raw imagery (potentially subject to misinterpretation) the data are first processed into meaningful analysis products, documented, and disseminated in a timely manner.
- The ability to classify the imaged oil signal into a high-resolution, GIS-compatible map of thickness classes is an important new asset for spill response and complements the use of SAR and SLAR data that do not have thickness quantification capabilities. For most response activities, however, it is sufficient to classify the oil films into just a few thickness categories, primarily separating sheen and very thin oil films from thicker accumulations. Response activities such as skimming, boom-towing, surfactant spraying, *in-situ* burning, and SCAT surveys are governed by actionable oil and are not likely to alter strategies based on

extremely precise knowledge of oil thickness variability. This fact significantly enhances the utility of aerial oil mapping systems under highly variable "real world" conditions that make absolute oil film thickness measurement extremely difficult.

- In addition to their utilization during actual spill response, the aerial image data provide unique, permanent documentation of oil spill patterns and events in spatial resolution generally not possible with visual survey-derived maps and records. This documentation can then be utilized for post-event analysis, injury assessment and research.
- For large spills, the limitations in imaging time due to acceptable sun angles and the cameras' relatively narrow field of view limit the aerial systems' utilization to specific areas or targets of interest, rather than for mapping of the entire spill. Visual aerial surveys done by trained observers likely remain much more time and cost-effective for frequent, rapid overviews of large spill events.
- The aerial imaging and subsequent oil-identification/characterization processing proved useful for both, offshore and shoreline response activities. In the case of mapping oiled vegetation, however, our experience suggests that detection of lightly oiled areas through direct detection of oil residue may be very difficult or impossible with the developed techniques. This capability could be potentially enhanced with the addition of a UV sensor and/or through indirect detection of changes in the plants' chlorophyll vigor.
- The relatively novel availability of the aerial multispectral imaging capabilities and analysis products in the DWH case resulted, especially in the beginning, in the potential underutilization of the information by some response groups and individuals who did not have the mechanism or infrastructure to use the data in their work protocols. As the availability of both satellite and aerial remote sensing becomes more commonplace during oil spill events, it is important to plan for and rehearse the inclusion of this type of information in response activities.

## Acknowledgments

The initial spill mapping system development work was funded by research grants from California Department of Fish & Game's Office of Spill Prevention and Response (OSPR) and the Bureau of Ocean Energy Management, Regulation, and Enforcement (formerly the US Minerals Management Service, presently Bureau of Safety and Environmental Enforcement). The operational use of the system during the DWH spill was funded by British Petroleum, with aircraft and pilot crew generously made available to OI by NOAA. We greatly thank BP's Robert M. Frost for his many contributions to this work, both during the response and during preparation of the manuscript.

## Disclaimer

The views expressed in this paper are solely those of the authors and do not represent the official views of the US Government, the State of California, or British Petroleum.

## References

- Alhina, K.G., M.A. Khan, A.E. Dabbagh, and T. Bader, 1993. Analysis of Landsat Thematic Mapper data for mapping oil slick concentrations - Arabian Gulf Oil-Spill 1991, *Arabian Journal for Science and Engineering*, 18(2):85-93.
- Belore, R.C., 1982. A device for measuring oil slick thickness, *Spill Technology Newsletter*, 7(2):44-47.
- Belore, R.C., K. Trudel, and J. Morrison, 2011. Weathering, Emulsification, and chemical dispersibility of Mississippi Canyon 252 crude oil: Field and laboratory studies, *Proceedings of the International Oil Spill Conference 2011*, 23-26 May, Portland, Oregon, unpaginated USB flash drive.

- Boggs, T., and R.B. Gomez, 2001. Fast hyperspectral data processing methods, *Proceedings of SPIE*, 4383, pp. 74–78.
- Bolus, R.L., 1996. Airborne testing of a suite of remote sensors for oil spill detecting on water, *Proceedings of the Second Thematic International Airborne Remote Sensing Conference and Exhibition*, 24–27 June, San Francisco, California, III:743–752.
- Bonn Agreement, 2007. *Bonn Agreement Aerial Surveillance Handbook*, Version 25, October 2007, URL: <http://www.bonnagreement.org/eng/doc/2007%20report%20on%20aerial%20surveillance.pdf> (last date accessed: 05 July 2012).
- Brekke, C., and A.H.S. Solberg, 2005. Oil spill detection by satellite remote sensing, *Remote Sensing of Environment*, 95:1–13.
- Brown, C.E., and M.F. Fingas, 2003. Review of the development of laser fluorosensors for oil spill application, *Marine Pollution Bulletin*, 47:477–484.
- Brown, C.E., and M.F. Fingas, 2005. Review of current global oil spill surveillance, monitoring and remote sensing capabilities. *Proceedings of the 28<sup>th</sup> Arctic and Marine Oil Spill Program (AMOP) Tech. Seminar*, 07–09 June, Calgary, Canada, pp. 789–798.
- C.E. Brown, M.F. Fingas, J-P. Monchalain, C. Neron, and C. Padioleau, 2005. Airborne oil slick thickness measurements: Realization of a dream, *Proceedings of the Eighth International Conference on Remote Sensing for Marine and Coastal Environments*, Ann Arbor, Michigan, 8 p.
- Byfield, V., 1998. *Optical Remote Sensing of Oil in the Marine Environment*, Ph.D. dissertation, University of Southampton, School of Ocean and Earth Science.
- Chouquet, M., R. Hedon, G. Vaudreuil, J-P. Monchalain, C. Padioleau, and R. H. Goodman, 1993. Remote thickness measurement of oil slicks on water by laser ultrasonics, *Proceedings of the 1993 International Oil Spill Conference*, 29 March-01 April 1993, Tampa, Florida, pp. 531–536.
- Clark, R.N., G.A. Swayze, I. Leifer, K.E. Livo, R. Kokaly, T. Hoefen, S. Lundeen, M. Eastwood, R.O. Green, N. Pearson, C. Sarture, I. McCubbin, D. Roberts, E. Bradley, D. Steele, T. Ryan, R. Dominguez, and the Airborne Visible/Infrared Imaging Spectrometer (AVIRIS) Team, 2010. *A Method for Quantitative Mapping of Thick Oil Spills Using Imaging Spectroscopy*, USGS Open-File Report, 2010-1167, 51 p.
- Davies, L., J. Corps, T. Lunel, and K. Dooley, 1999. *Estimation of Oil Thickness*, AEA Technology Report, AEAT-5279(1), 34 p.
- Fingas, M.F., and C.E. Brown, 1997. Review of oil spill remote sensing, *Spill Science & Technology Bulletin*, 4(4):199–208.
- Fingas, M.F., and C.E. Brown, 2011. Oil Spill Remote Sensing: A Review, *Oil Spill Science and Technology: Prevention, Response, and Clean Up* (M. Fingas, editor), Elsevier, Burlington, Massachusetts, pp. 111–169.
- Goodman, R., and C.E. Brown, 2005. Oil detection limits for a number of remote sensing Systems, *Proceedings of the Eighth International Conference on Remote Sensing for Marine and Coastal Environments*, 18–19 May, Altarum Conferences, Halifax, Nova Scotia, 8 p.
- Hengstermann, T., and R. Reuter, 1990. Lidar fluorosensing of mineral oil spills on the sea surface, *Applied Optics*, 29(22):3218–3227.
- Hornstein 1972. *The Appearance and Visibility of Thin Oil Films on Water*, U.S. Environmental Protection Agency, Report EPA-R2-72-039, Cincinnati, Ohio.
- Hu, C., L. Xiaofeng, W.G. Pichel, and F.E. Muller-Karger, 2009. Detection of natural oil slicks in the NW Gulf of Mexico using MODIS imagery, *Geophysical Research Letters*, 36, L01604, doi:10.1029/2008GL036119.
- Hurford, N., 1989. Review of remote sensing technology, *The Remote Sensing of Oil Slicks* (A.E. Lodge, Editor), John Wiley and Sons, Chichester, UK, pp. 7–16.
- Jha, M.N., J. Levy, and Y. Gao, 2008. Advances in remote sensing for oil spill disaster management: State-of-the-art sensors technology for oil spill surveillance, *Sensors*, 8:236–255.
- Lehr, W. 2010. Visual Observation and the Bonn Agreement, *Proceedings of the Thirty-third Arctic and Marine Oilspill Technical Program Technical Seminar*, Environment Canada, Ottawa, Ontario), pp. 669–678.
- Lennon, M., S. Babichenko, N. Thomas, V. Mariette, G. Mercier, and A. Lisin, 2006. Detection and mapping of oil slicks in the sea by combined use of hyperspectral imagery and laser induced fluorescence, *EARSel eProceedings*, 5:1–9.
- NOAA, 2011. URL: <http://response.restoration.noaa.gov/oil-and-chemical-spills> (last date accessed: 05 July 2012).
- Rogne, T., I. Macdonald, A. Smith, M.C. Kennicutt, and C. Giammova, 1993. Multispectral remote sensing and truth data from the Tenyo-Maru oil spill, *Photogrammetric Engineering & Remote Sensing*, 59(3):391–397.
- Rouse, J.W., R.H. Haas, J.A. Schell, and D.W. Deering, 1973. Monitoring vegetation systems in the Great Plains with ERTS, *Proceedings of the Third ERTS Symposium*, NASA SP-351, I:309–317.
- Svejkovsky, J., and J. Muskat, 2006. Real-time detection of oil slick thickness patterns with a portable multispectral sensor, *Final Report for U. S. Minerals Management Service Contract 0105CT39144*, 37 p.
- Svejkovsky, J., J. Muskat, and J. Mullin, 2008. Mapping oil spill thickness with a portable multispectral aerial imager, *Proceedings of the International Oil Spill Conference 2008*, 04–08 May, Savannah, Georgia, unpaginated USB flash drive.
- Svejkovsky, J., and J. Muskat, 2009. Development of a portable multispectral aerial sensor for real-time oil spill thickness mapping in coastal and offshore waters, *Final Report for U. S. Minerals Management Service Contract M07PC13205*, 33 p.
- Trieschmann, O., T. Hunsenger, L. Tufte, and U. Barjenbruch, 2003. Data assimilation of an airborne multiple remote sensor system and of satellite images for the North and Baltic Sea, *Remote Sensing of the Ocean and Sea Ice* (C.R. Boastater, Jr. and R. Santoleri, editors), SPIE, Bellingham, Washington, pp. 51–60.
- Zielinski, O., 2003. Airborne pollution surveillance using multi-sensor Systems, *Sea Technology*, 44:28–32.

(Received 10 August 2011; accepted 13 December 2011; final version 06 February 2012)